



LUND
UNIVERSITY

IMPLEMENTATION OF REACTION KINETICS INTO REACTOR MODEL FOLLOWED BY VALIDATION OF THE REACTOR MODEL

MASTER THESIS | DEPARTMENT OF CHEMICAL ENGINEERING | 2021



Implementation of Reaction Kinetics into Reactor Model Followed by Validation of the Reactor Model

by

Rebecka Svensson

Department of Chemical Engineering

Lund University June 2021

Supervisor: Senior Lecturer Helena Svensson

Co-supervisor: Process Engineer Larissa Cunico

Examiner: Professor Ola Wallberg

©2021 by Rebecka Svensson. All rights reserved.
Printed in Sweden, Media-Tryck Lund University.
Photographer front page: Kennet Ruona.

Implementering av reaktionskinetik till reaktormodell samt validering av reaktormodellen

Preface

This work described in this master thesis has been performed at the department of Chemical Engineering at Lund University in collaboration with Johnson Matthey Formox AB in Perstorp. The master thesis was a project including both the research and development department as well as the process department in Perstorp. The work for the master thesis has been performed partly at the office in Perstorp and partly at the home office.

I would like to thank the company, Johnson Matthey, for giving me the opportunity to do my master thesis at their company. It has been an honor to be part of this internal project and it has been a great experience for me. Especially I would like to thank my supervisor at Johnson Matthey, Larissa Cunico, who helped me a lot with the different parts in the project. I appreciate all the time and effort you spent on this project.

When writing and structuring the report, Helena Svensson, my supervisor at the university, has been very supportive and given me a lot of valuable feedback and support. Thank you.

Finally I would like to thank my friends and family, for being very supportive during this exciting and intensive period this spring.

Rebecka Svensson, June 2021, Lund

Abstract

This master thesis project was performed in collaboration with Johnson Matthey. Johnson Matthey is a worldwide company working with sustainable technologies. The site in Perstorp, where this work was performed, focus on formaldehyde production. In order to continuously improve chemical processes, simulation and modeling are advantageous tools. They can give a better understanding of the processes and the optimum operation conditions. By using reactor modeling, design improvements can be investigated, and the efficiency of the plant can be increased.

The aim with this project was to implement a kinetic model into an existing reactor model and to further on validate the reactor model against data from the pilot reactor. The model was developed in Aspen Custom Modeler.

The kinetic model was described by the power law, but at an early stage, numerical errors were obtained with this kinetic model. The power law equations were replaced with another kinetics model from literature. The kinetic model from literature was more complex and more equations were added, including the surface fraction of the components. The development of the kinetic model was an ongoing project and two kinetic models were developed from the literature kinetic model. The rebased model including a reference temperature and the second one with refitted parameters to the experimental data provided from Johnson Matthey.

The rebased model was validated against the pilot reactor and the outlet composition and temperature were compared. The results showed deviation when compared with the pilot plant data, with relative deviation for the temperature profile of +15% and relative deviation for the outlet composition of +2.6% for formaldehyde. A possible explanation for the deviation could be higher reaction rates for reaction 1 and 2. However, the reactor model showed similar behaviour of the pilot plant data regarding the hot spots and similar range of concentration for the main components in the outlet, which shows great potential describing the pilot plant in the future after final validation.

The different layers of catalyst along the tube were implemented in the reactor model and the inert dilution was taking into consideration. When analysing the result in the radial direction, the reactor model showed expected results for the composition and temperature, i.e. constant values for the composition in the radial direction and warmer temperature in the center of the tube in comparison to the wall. This result indicates that the kinetic model was successfully implemented in 2D.

To improve the reactor model, the refitted kinetic model can be evaluated further. This kinetic model with refitted parameters showed problems with convergence and due to the time limit of this project, the convergence problem could not be solved. The mass transfer limitation within the catalyst particle should preferably be implemented as well in order to describe the correct behaviour in the reactor tube.

Sammanfattning

Detta examensarbete utfördes i samarbete med Johnson Matthey. Johnson Matthey är ett globalt företag som arbetar med hållbara teknologier. Siten i Perstorp, där detta arbete utfördes, fokuserar på formaldehydproduktion. För att kontinuerligt förbättra kemiska processer, används verktyg så som simulering och programmering. Dessa verktyg ger en bättre förståelse av processen och dess optimala produktionsförhållanden. Genom att använda modellering, kan designen av en process förbättras och effektiviteten kan ökas.

Syftet med detta examensarbete var att implementera en kinetikmodell i en redan existerande reaktormodell och att vidare validera denna reaktormodell gentemot pilotreaktorn. Modellen var utvecklad i Aspen Customer Modeler.

Den kinetiska modellen var beskriven enligt "power law", men i ett tidigt skede upptäcktes numeriska fel med denna kinetikmodell. Den befintliga kinetikmodellen byttes ut mot en annan kinetisk modell från litteraturen. Denna modell var betydligt mer komplex. Utvecklingen av kinetikmodellen pågick parallellt med detta projekt och den kinetiska modellen från litteraturen utvecklades med en referenstemperatur samt anpassades till experimentell data från Johnson Matthey.

Den nya kinetiska modellen med referenstemperatur validerades gentemot pilotreaktorn och sammansättningen i utflödet samt temperaturen undersöktes. Resultatet visade en avvikelse på +15% för temperaturprofilen och +2.6% för sammansättningen av formaldehyd i utflödet. En möjlig förklaring till detta resultat är en högre reaktionshastighet, för reaktion 1 och 2, än förväntat. Resultatet från reaktormodellen uppvisade ett liknande beteende i jämförelse med pilotreaktor och har stor potential att beskriva pilot reaktorn efter ytterligare utveckling samt slutgiltig validering.

De olika lagrena av katalysator längst reaktortuben var implementerade och reaktormodellen tog även hänsyn till utspädningen med inert. Undersökning av sammansättningen i utflödet och temperaturen vid olika axiella punkter påvisade ett förväntat resultat där sammansättningen var konstant och i den axiella riktningen och temperaturen minskade från mitten av reaktortuben ut till väggen. Detta indikerar att den kinetiska modellen var korrekt implementerad i 2D.

För att förbättra reaktormodellen måste versionen anpassad till experimentell data från Johnson Matthey, valideras ytterligare. Denna kinetiska modell hade problem att konvergera och på grund av den begränsade tiden för detta projekt, kunde inte detta problem lösas. Masstransporten i katalysatorpartiklarna bör också adderas till reaktormodellen för att förbättra dess prestanda.

Contents

1	Introduction	1
1.1	Aim	1
1.2	Main Objectives	1
2	Background	1
2.1	Formaldehyde	2
2.2	The FORMOX Process	2
2.3	Catalyst	4
2.3.1	Catalyst Activity Profile	4
2.4	Aspen Custom Modeler	5
2.5	Existing Reactor Model	5
3	Theory	6
3.1	Modeling	6
3.2	Reactions	7
3.3	Catalyst Technology	8
3.3.1	Water Inhibition	9
3.4	Experimental Data to Develop Intrinsic Kinetics	9
3.5	Reaction Mechanisms	10
3.5.1	Langmuir-Hinshelwood	10
3.5.2	Mars van Krevelen	11
3.6	Mass Transfer	11
3.6.1	Internal Mass Transfer Limitations	12
3.6.2	External Mass Transfer Limitations	13
3.7	Heat Transfer	13
3.7.1	Internal Heat Transfer Limitations	13
3.7.2	External Heat Transfer Limitations	14
3.8	Power Law Kinetics	14
3.8.1	Development of Intrinsic Kinetic Model	14
3.9	Deshmukh Kinetic Model	15
3.10	Pilot Plant Reactor	19
4	Method	20
4.1	Modeling Set Up	20
4.1.1	Troubleshooting	21
4.1.2	Running Mode	21
4.1.3	Obtained Results	21
4.2	Verification of Calculation Method	21
4.3	Implementation of Kinetic Model	22
4.3.1	Implementation of Power Law	22
4.4	Parameters	23
4.4.1	Inlet Composition	23
4.4.2	Tube Density	23
4.4.3	Bed Geometric Surface Area	23
4.4.4	Inlet Composition	23

4.5	Implementation to Reactor Model	24
4.6	Implementation of Heat and Mass Transfer Limitations	24
4.7	Validation Against Pilot Plant	24
4.7.1	Input Parameters from Pilot Reactor	25
4.7.2	Different Layers of Catalyst	25
5	Result and Discussion	25
5.1	Development and Implementation of Kinetic Models	26
5.1.1	Power Law	26
5.1.2	Refitted Power Law	26
5.1.3	Deshmukh Kinetic Model	28
5.1.4	Rebased and Refitted Kinetic Model	31
5.2	Reactor Model	32
5.2.1	Convergence Problem in Steady State	32
5.2.2	Validation of Rebased Model Against Pilot Plant	33
5.2.3	Validation of Rebased Model Against Pilot Plant with Modified Reaction Rate	37
5.2.4	Validation of 2D model	41
5.3	General Discussion	44
6	Conclusion	45
6.1	Future Work	46
	References	47

Nomenclature

$(\Sigma\nu)_i$	Diffusion volume of component i	$\frac{m^3}{mol}$
$\Delta H_{r,k}$	Heat of reaction	$\frac{J}{mol}$
ϵ_p	Catalyst porosity	—
$\lambda_{eff,p}$	Effective radial bed thermal conductivity	$\frac{W}{mK}$
ν_i	Stoichiometric coefficient for component i	—
ρ_{pellet}	Density of the catalyst pellet	$\frac{kg}{m^3}$
ρ_{tube}	Tube density	$\frac{kg}{m^3}$
τ_p	Catalyst pore tortuosity	—
θ_i	Surface fraction of component i	—
a	Specific catalyst interfacial area	m^2
a'	Specific external surface area of one pellet	m^2
a_v	Specific external surface area of a single catalyst particle	$\frac{m^2}{m_{pellet}^3}$
A_{cat}	Surface area of the catalyst	m^2
c_b	Bulk concentration of reactant methanol	$\frac{mol}{m_{gas}^3}$
c_s	Concentration of reactant methanol at the external pellet surface	$\frac{mol}{m_{gas}^3}$
$C_{a,in}$	Molar concentration of A at the inlet	$\frac{mol}{m_{gas}^3}$
$C_{a,out}$	Molar concentration of A in the outlet	$\frac{mol}{m_{gas}^3}$
d_p	Characteristic diameter	m
$D_{A,eff}$	Effective diffusivity for component A	$\frac{m^2}{s}$
$D_{A,k}$	Knudsen diffusivity for component A	$\frac{m^2}{s}$
D_{AB}	Molecular diffusivity	$\frac{m^2}{s}$
E_a	Activation energy	$\frac{J}{mol}$
f	Molar flux	—
$F_{A,0}$	Molar flow of feed	$\frac{mol}{s}$
GSA	Bed geometric surface area	$\frac{m^2}{m^3}$
h	Gas-solid heat transfer coefficient	$\frac{W}{m^2K}$

k_f	Mass transfer coefficient	$\frac{m}{s}$
k_g	External mass transfer coefficient	$\frac{m}{s}$
K_i	Adsorption constant for component i	—
k_s	Gas to catalyst mass transfer coefficient	$\frac{m}{s}$
$K_{0,i}$	Pre-exponential factor for component i	—
$K_{eq,i}$	Equilibrium constant for reaction i	—
$k_{n,0}$	Frequency factor for reaction n	—
k_n	Rate constant for reaction n	—
m_i	Molecular mass of i	$\frac{kg}{mol}$
m_{pellet}	Weight catalyst pellet	kg
n_i	Molar flow for component i	$\frac{mol}{min}$
n_{tot}	Total molar flow	$\frac{mol}{min}$
p_i	Partial pressure of component i	—
$P_{g,i}$	Partial pressure for component i	—
$P_{g,tot}$	Total gas pressure	Pa
R	Gas constant	$\frac{J}{molK}$
r_i	Reaction rate for reaction i	$\frac{mol}{m^2s}$
r_{ave}	Average pore radius	m
r_{inner}	Tube inner radius	m
r_{outer}	Tube outer radius	m
$R_{V,A}^{obs}$	Observed volumetric reaction rate per unit of catalyst pellet volume	$\frac{mol}{m^3_{pellet}s}$
s_i	Formation rate of component i	$\frac{mol}{m^2s}$
T_b	Temperature in the catalyst bed	K
T_{ref}	Reference temperature	K
V_{pellet}	Volume of the catalyst pellet	m^3
x_i	Molar fraction	$mol\%$
$z_{g,in}$	Average molar fraction of i in the gas	$mol\%$

1 Introduction

This report will account for the master thesis work performed in collaboration with Johnson Matthey Formox AB to develop a reactor model. Johnson Matthey is a worldwide company working with sustainable technologies. The site in Perstorp, Johnson Matthey Formox AB, focus on formaldehyde production. Formaldehyde is an important chemical intermediate and new production plants are commissioned every year [1]. Johnson Matthey Formox AB work with the design of formaldehyde plants, technical support as well as the development and manufacturing of the catalyst.

In order to continuously improve chemical processes, simulation and modeling are advantageous tools. They can give a better understanding of the processes and the optimum operation conditions. By using reactor modeling, design improvements can be investigated, and the efficiency of the plant can be increased. Some other advantages of modeling and simulation are the ability to provide more customized services to the customers, facilitate troubleshooting the processes, and to help reducing the operating costs of the plants.

1.1 Aim

The aim with this master thesis was to explore the catalyst kinetics in a formaldehyde reactor and to implement a kinetics model into the reactor model. The kinetics model was developed separately and was further implemented to an existing reactor model. A well developed reactor model could be used to further improve the reactor development. The model will further on be used inside the company to predict the reactor performance for parameters such as composition of major and minor products and reaction temperatures. The reactor model aims to evaluate the reactor design as well as the catalyst aging. A well developed reactor model is also useful for predicting the effect of recycled streams, and the possibility to use alternative feedstocks.

1.2 Main Objectives

The main objectives of this master thesis was to implement a kinetics model into the existing reactor model and validate it against the pilot plant reactor. Beyond this, the objective with the project was to discuss and answer the following questions.

- What kinetic model describes the pilot reactor best?
- How well was the reactor model with the implemented kinetics representing the pilot plant reactor?

2 Background

In this section, the background knowledge for this project will be presented. It includes a brief introduction to the intermediate chemical formaldehyde, the tech-

nology of the **FORMOX**TM process and the catalyst technology used in the **FORMOX** processes.

2.1 Formaldehyde

Formaldehyde is an organic chemical, discovered in 1859 by Butlerov. The commercial production of formaldehyde started in the beginning of the twentieth century and it has become one of the most important industrial chemicals in the world. The two main processes used to produce formaldehyde is the silver catalyst process and the oxide process. [1]

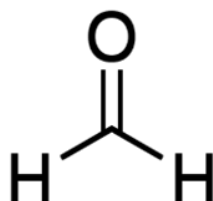


Figure 1: Chemical structure of formaldehyde, from Sigma-Aldrich, 2021 [2].

Formaldehyde is a colorless gas at room temperature. As seen in Figure 1, the formaldehyde molecule is quite small, and it is highly reactive. Due to its high reactivity, it is further used in a lot of different industries, and can be defined as a chemical intermediate. Formaldehyde is usually stored in a solution with water, this solution is called formalin and can be produced containing different concentrations of formaldehyde. Solutions of formaldehyde are unstable, which can result in formation of paraformaldehyde and formic acid. The reactions to paraformaldehyde and formic acid increase with time and temperature and it is therefore difficult to store formalin. Due to the instability of the solution, transportation of the product aims to be minimized. The formaldehyde plant is usually placed next to the industrial plant where the formalin is needed. [1]

Formaldehyde and water solution, formalin, is mainly used in the wood and chemical industry where it can be used for e.g. coatings, adhesive, and fertilizers.

2.2 The FORMOX Process

As mentioned above in *2.1 Formaldehyde*, the product formaldehyde can be produced by two different processes, the silver catalyst process and the oxide process. Johnson Matthey is working with the oxide process, also known as the **FORMOX** process. The technology behind the **FORMOX** process has been known for a long time, the oxidation of methanol with an iron–molybdenum oxide catalyst was patented already in 1933. The first commercial oxide process using iron-molybdenum oxide catalyst was put into operation in 1952. [1]

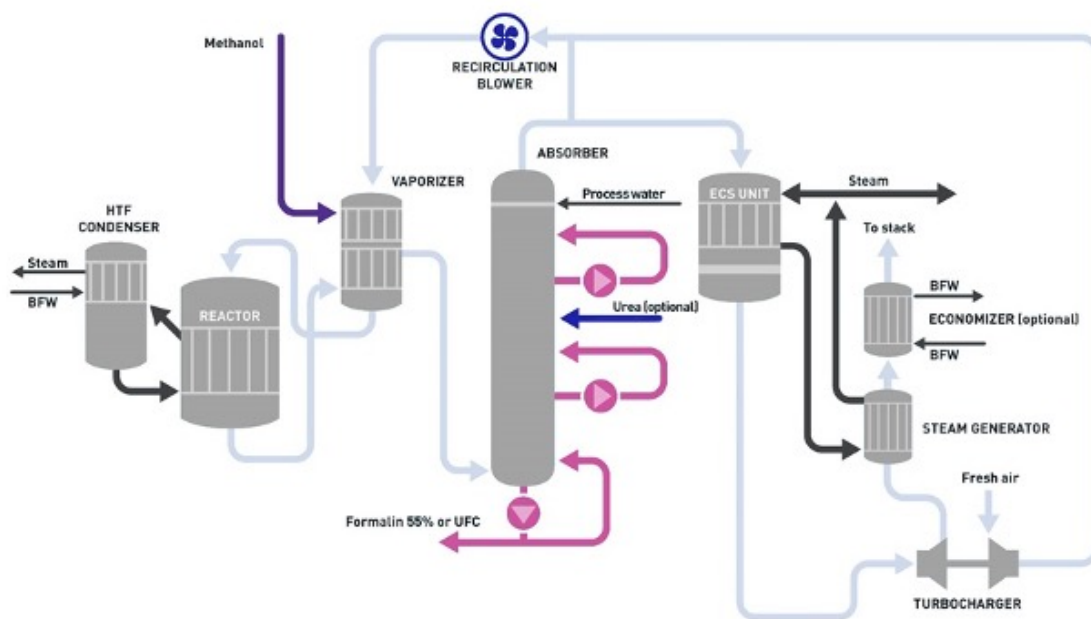


Figure 2: Schematic flowsheet of the **FORMOX** 2.0 process from Johnson Matthey, 2021 [3].

Figure 2 shows a flowsheet of the **FORMOX** 2.0 process. Unlike the older **FORMOX** process with a pressurization blower, the inlet air is pressurized with a turbocharger. This makes it possible to use a higher pressure in the plant and it also decrease the energy consumption of the plant [3]. The pressurization of the original **FORMOX** plant is 0.5 barg and with the turbochargers the pressure can reach 1.0 barg [3].

As seen in Figure 2, the pressurized air and the inlet methanol are transported into the vaporizer. The vaporized feed enters the tubular reactor filled with catalyst and the exothermic main reaction forms formaldehyde and water. Due to the exothermic reactions inside the tube, the temperature reaches 300-400°C in the reactor. A heat-transfer fluid outside the tubes control the heat inside the tubes to avoid hot spots. Additional by-products are formed along the tube, dimethyl ether (*DME*), carbon monoxide (*CO*), dimethoxy methane (*DMM*), methyl formate (*MF*) and carbon dioxide (*CO*₂) [3]. A methanol conversion greater than 99% can be reached by the **FORMOX** process and the overall yield is generally between 88-92% [1]. The formaldehyde product from the reactor is transferred to the absorber where water is added to obtain a lower concentration of formaldehyde. This product with formaldehyde and water is called formalin and the formaldehyde concentration varies between 37-55wt-% in the formalin product [1]. The formalin product leaves the absorber at the bottom of the column. The gas stream, leaving the absorber at the top, enters the emission control reactor to decrease the level of toxic gases before leaving the plant as a flue gas [3].

2.3 Catalyst

A mixed phase catalyst consisting of $MoO_3/Fe_2(MoO_4)_3$ is used in the oxide process when producing formaldehyde. Due to the excess of molybdenum, the catalyst has a lower activity, which increases the selectivity. The physical structure of the catalyst is ring shaped and can be described as a hollow cylinder. The geometry of a pellet is illustrated in Figure 3.



Figure 3: Illustration of the pellet geometry.

This shape of the catalyst, allows the gas flow through the reactor tubes to be increased due to the hole in the particle. This is an important factor that affects the productivity. Another factor that affects the productivity is the diluted layer of catalyst in the top of the reactor tube. The process reaches a selectivity of 95% and the selectivity decreases to 92% with the aging of the catalyst. Aging of $MoO_3/Fe_2(MoO_4)_3$ is due to the formation of volatile methoxy-hydroxy-molybdenum. The production costs of formaldehyde are mainly based on the cost of methanol and a high selectivity is favorable in order to minimize the consumption of methanol [4]. In order to determine the activity and the degree of aging of the catalyst, the molybdenum loss can be modeled. The loss of MoO increases with higher concentration of methanol and higher temperatures. [5]

2.3.1 Catalyst Activity Profile

In each reactor tube, catalyst pellets are loaded. The catalysts are loaded in a certain way to obtain optimized reactor conditions such as temperature profiles and optimized mass flow rate. It can be different catalysts at different heights along the reactor tube. It is common to dilute the catalysts with inert pellet. The catalyst activity describes how the catalysts behave along the tube. Dependent of the loading plan in the reactor tube, the catalyst activity profile changes. [6].

2.4 Aspen Custom Modeler

To create the model for the reactor kinetics, Aspen Custom Modeler version 10 (ACM) was used. ACM is a custom modeler tool where models can be created and simulations can be performed. It is also possible to further transfer the model into Aspen Plus for simulation and combine it with other unit operations already developed. When the model, created in ACM, is used in Aspen Plus, it will be generated as a reactor block, possible to add to the flowsheet.

A model created in ACM, consists of a main code and additional functions, called procedures. The model is built with one or several procedures and one main code. The programming language used in the main code is optional. The procedures are called in the main code and all the differential equations are solved in the main code. In the procedure code, the programming language Fortran must be used since the code is generated through a Fortran Compiler. [7] The procedures are used as built-in mathematical equation solvers and the system is not solving the equations in a sequence, line by line. The inputs are convenient changed in the main code and the same set of equations are used in the procedure. [8]

2.5 Existing Reactor Model

A reactor model has been developed internally at Johnson Matthey by Manufacturing Research Engineering Lead Darren Gobby and Principal Engineer Mike Davies. As mention above in *2.4 Aspen Custom Modeler*, a model consists of a main model and additional procedures. The procedures describe the molar enthalpy, the reaction enthalpy, the molecular weight, and the reaction rate. The procedure describing the reaction rate was implemented as pseudo kinetics and was a placeholder until a new kinetic model is to be implemented. The external mass and heat transfer limitations are described in the existing reactor model.

This master thesis project focused on implementing a kinetic model into the procedure calculating the reaction rate in the existing reactor model. The reactor model is defined as the whole code including main code and procedures. A kinetic model is the specific equations implemented in the procedure describing the reaction rate. In Figure 4 below, the structure of the reactor model is illustrated and it is also illustrated where the kinetic model was implemented.

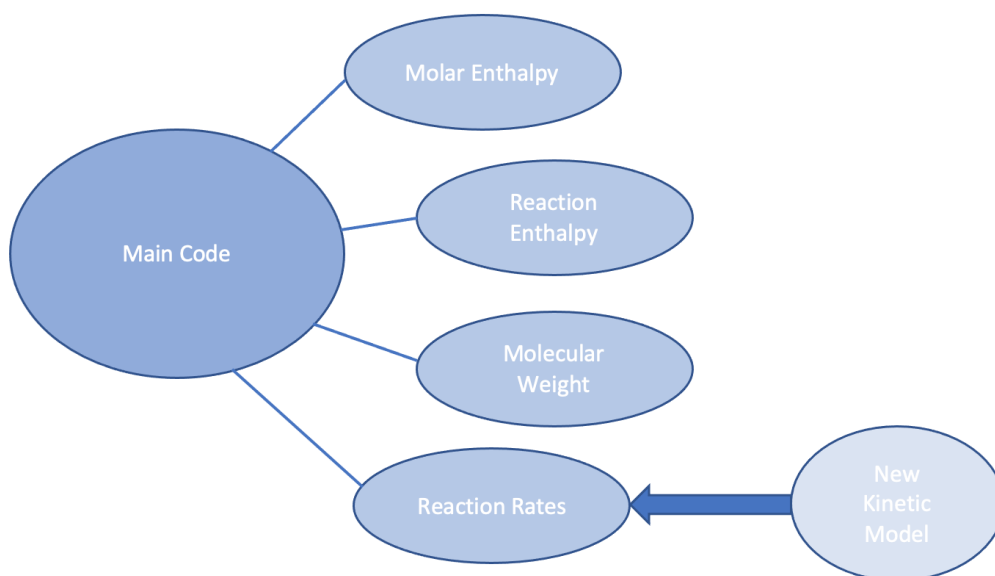


Figure 4: Structure of the reactor model and where the kinetic model was implemented.

This master thesis was part of a bigger project going on inside Johnson Matthey. Robert Gallen, Senior Scientist, was working with the improvement of the kinetics and the regression of the parameters. The kinetic model was updated a couple of times during the semester, to improve the robustness and the kinetic model itself.

3 Theory

This section includes the literature study performed before the kinetic model was implemented. The reactions and the reaction mechanisms in a **FORMOX** reactor are described below, as well as the kinetics and additional information regarding the catalyst.

3.1 Modeling

The objective when developing a model is to create a simplified version of a real phenomenon and validate the model against the real plant, aiming to describe the plant as accurately as possible. An illustration of the general concept of modeling is shown in Figure 5 [9]. Depending on the limitations the model has, the model is more or less abstract. Modeling can be explained as consisting of three main steps; model design, implementation and validation [9]. This project started at the second step, to complete the implementation and the validation of the model.

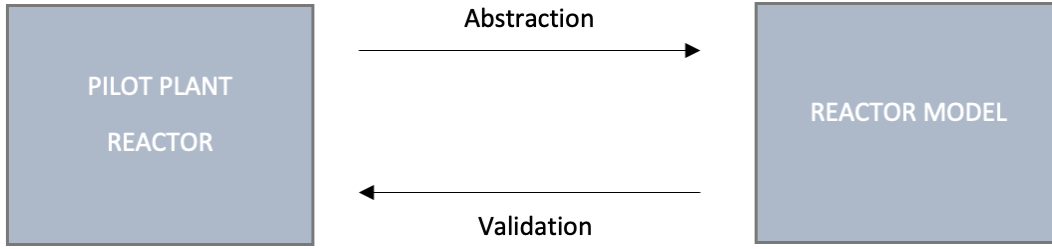
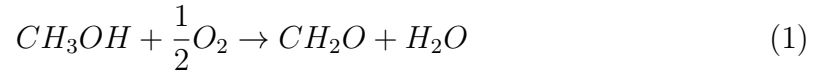


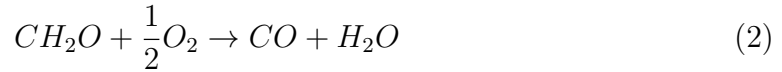
Figure 5: Illustration of the modeling phenomena, inspired by Höst et al. 2006 [9]

3.2 Reactions

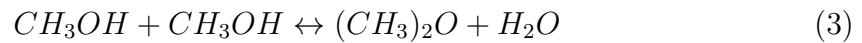
According to literature [10], there are seven reactions taking place along the tube in the reactor, forming the main product formaldehyde and some side products. The main reaction in the reactor is the exothermic reaction where methanol is partially oxidized to formaldehyde and water. The methanol oxidation is described in reaction 1 [10].



Formaldehyde can be further oxidized to form the by-product CO , shown in reaction 2 [10].



Methanol can react with itself and form the side product DME according to reaction 3. The reaction can be described as an equilibrium reaction [10].



DME can react further and form formaldehyde according to reaction 4 [10].



When formaldehyde is formed, it can react with methanol and two side reactions occurs forming DMM and MF [10]. The side reactions are described below in reaction 5 and reaction 6.





CO can react further and form CO_2 according to reaction 7.



The correlations between the different reactions is illustrated in the reaction scheme shown in Figure 6.

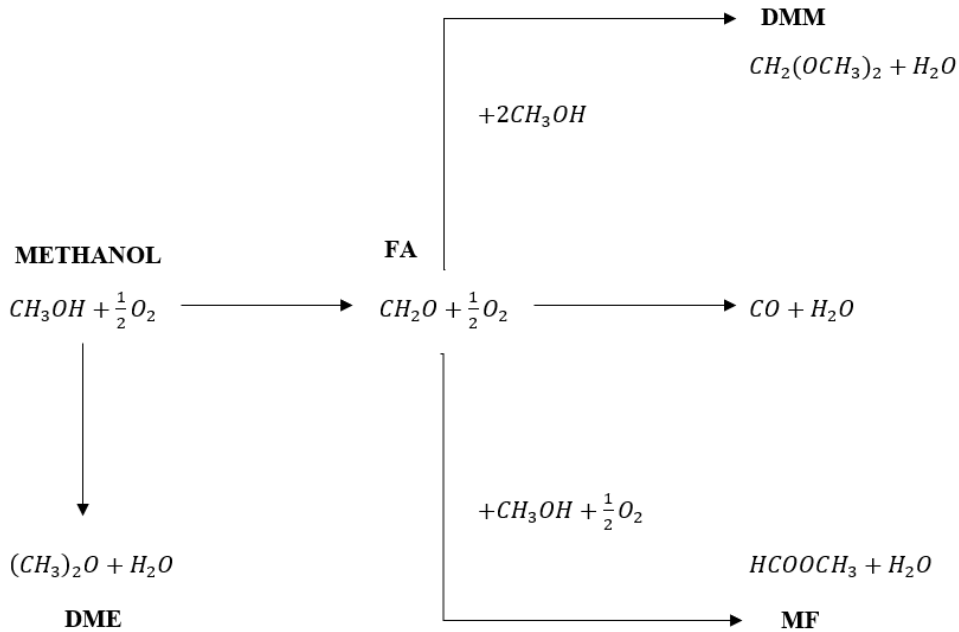


Figure 6: A possible description of the reactions occurring in the **FORMOX** reactor, inspired by Deshmukh [10].

In the illustration above, all the reactions are shown as forward reactions only. As seen in reaction 3, the *DME* production can be considered as an equilibrium reaction. Reaction 5 can also be considered as an equilibrium reactions [10].

3.3 Catalyst Technology

The mechanism describing a heterogeneous gas-solid catalyst reaction consists of five steps [11].

1. Mass transfer of reactant to catalyst surface.
2. Adsorption of reactants onto catalyst active site.
3. Catalytic reaction.

4. Desorption of reaction product from catalyst active site.
5. Mass transfer of product away from catalyst surface.

To achieve an optimized catalyst activity, with high conversion and stable temperature, and to maintain a uniform temperature inside the reactor, different catalyst activity profiles (CAP) are used. Inert ceramic rings with larger particle size are used as the top layer to decrease the pressure drop along the tube. [6] [13]

3.3.1 Water Inhibition

It has been shown that low concentrations of water and low temperatures inhibits the formation of formaldehyde due to catalyst adsorption. The water adsorbs competitively and will inhibit the methanol to adsorb to the active sites at the catalyst. This is likely due to the chemical difference between water and methanol, since water has a higher basicity than methanol, it is more likely to adsorb to active sites with higher acidity. When the concentration of water increases along the tube, the selectivity to FA is increased and the selectivity to form side products *DME* and *DMM* is decreased. The decreased selectivity of *DME* and *DMM* can also be explained by the inhibition of the active sites which decreases the oxidation of methanol to *DME* and formaldehyde to *DMM* [12]. The gas phase equilibrium between formaldehyde and *DMM* can also be an explanation of why the amount of *DMM* decreases [10].

3.4 Experimental Data to Develop Intrinsic Kinetics

The rate expressions used for the kinetic model, described in *3.8.1 Development of Intrinsic Kinetic Model* are regressed from experimental data measured by Schmidt [13]. The experimental study performed by Schmidt [13] collected a data set for developing the rate expressions for the reactions, aiming to create a kinetic model. The reaction kinetics are validated for an aluminum reactor tube with an inert layer of ceramic rings followed by a mixed layer of catalyst. The catalyst and the inert are crushed and sieved to a grain size of 212-250 μm . The experiments were performed between approximately 260-280°C. The experimental measurements were performed as a master thesis project by Manfred Schmidt. [13]

The reactor where the kinetic data were measured, is a small-scale reactor built in the Johnson Matthey laboratory in Perstorp. A cross sectional picture is shown in Figure 7 to illustrate the reactor tube and the catalyst load [13].

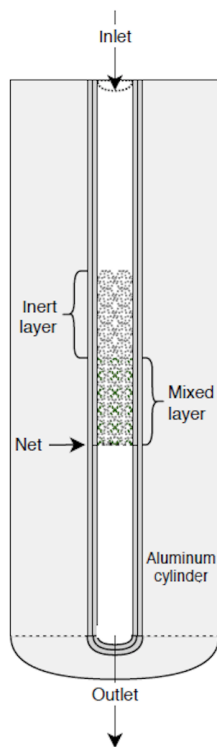


Figure 7: Cross section of the small-scale reactor, illustrated by Manfred Schmidt [13].

Due to a leak when performing the experiment, the conversion was higher than recommended for intrinsic kinetics testing (10%). The leak was identified on the feed line and the result may be affected by the mass and heat transfer limitations. [13]

3.5 Reaction Mechanisms

When a reaction takes place, it can be described by a reaction mechanism. Two common reaction mechanisms describing the behaviour of the catalyst reaction are presented in this section, Langmuir-Hinshelwood and Mars van Krevelen.

3.5.1 Langmuir-Hinshelwood

Langmuir-Hinshelwood is a reaction mechanism and describes how the reaction on the catalyst occurs. The mechanism assumes that the reactant adsorbs to the active site on the catalyst, react at the surface and afterwards desorb from the catalyst active site. The reaction is limited by the surface adsorption on the surface of the catalyst. The Langmuir-Hinshelwood isotherm is valid for catalysts with only one type of active site. The mechanism is illustrated in Figure 8, for reaction 1. [14]

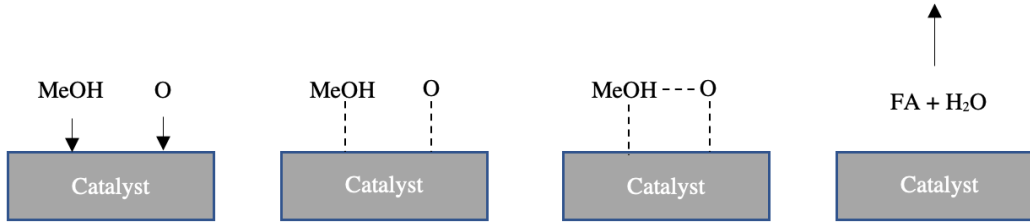
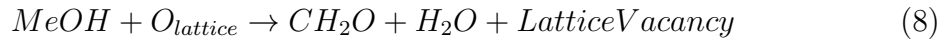


Figure 8: Reaction 1 described with reaction mechanism Langmuir-Hinshelwood.

3.5.2 Mars van Krevelen

Another way to describe a reaction mechanism is by the Mars van Krevelen rate expression. The Mars van Krevelen rate expression is only valid for reactions where oxygen is included and adsorbed to a single site. In the Mars van Krevelen model, the redox catalyst is assumed to be a part of the reaction. The reactant in the gas phase e.g methanol, will react with the oxygen in the catalyst lattice and form formaldehyde. When the oxygen and methanol have reacted, oxygen from the gas phase adsorb to the vacancy in the catalyst lattice and the lattice is complete again. The catalytic reaction between methanol and oxygen can be described as in reaction 8 and reaction 9. [15]



As seen in the reactions above, the methanol adsorb to the catalyst surface and react with the oxygen in the catalyst lattice. When the lattice vacancy occur, the oxygen in the gas phase react with the catalyst and fill the vacancy in the lattice. [15]

3.6 Mass Transfer

In order to develop an intrinsic kinetic model, mass transfer limitations aim to be decreased as much as possible. An experimental study has been done at Johnson Matthey Formox AB to evaluate how their catalysts affect the internal and external mass transfer. The result from this study shows no indications of internal nor external mass transfer limitations within the operating ranges [12].

The internal and external diffusion paths are illustrated in Figure 9. The external diffusion from the bulk through the gas film, and the internal diffusion through the catalyst pores [16].

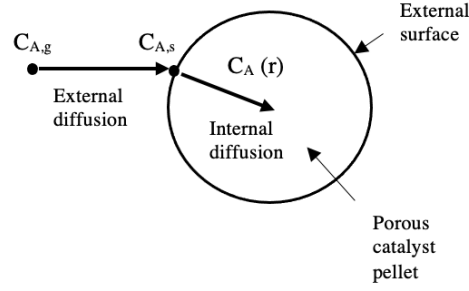


Figure 9: Mass transfer steps for a catalyst pellet, inspired by Fogler 2017 [16].

The external and internal mass transfer limitations for a fixed bed reactor are described in the following equations.

3.6.1 Internal Mass Transfer Limitations

The correlation Wheeler-Weisz is used to determine the intraparticle mass transfer limitation caused by diffusion inside the catalyst. The correlation is shown below in equation 10. The resistance due to internal diffusion have to be less than 15% to avoid internal mass transfer limitations. n describes the reaction order. [17]

$$\frac{R_{V,A}^{obs} (d_p/6)^2}{D_{A,eff} c_s} \frac{n+1}{2} < 0.15 \quad (10)$$

The reactant A diffuses from the catalyst surface with higher concentration into the pores, containing a lower concentration. The effective diffusivity coefficient $D_{A,eff}$, describes the average behaviour inside the pores, since the pores are not ideal shaped and the cross-sectional area differs inside the pellet [16]. To determine the effective diffusivity, equation 11 can be used [17].

$$D_{A,eff} = \frac{\epsilon_p / \tau_p}{\frac{1}{D_{AB}} + \frac{1}{D_{A,k}}} \quad (11)$$

The molecular diffusivity D_{AB} , also known as the bulk diffusivity, describes the collision between molecules in the gas phase. It can be calculated with the expression shown in equation 12 [17].

$$D_{AB} = \frac{3.2 \times 10^{-11} T^{1.75} \sqrt{\frac{1}{m_A} + \frac{1}{m_B}}}{P_{tot} \left\{ (\Sigma \nu)_A^{1/3} + (\Sigma \nu)_B^{1/3} \right\}^2} \quad (12)$$

Knudsen diffusion describes the internal diffusion where the gas molecules are limited by the collision between the molecules and the pore walls. The Knudsen diffusivity coefficient used in equation 11 can be calculated as shown below in equation 13 [17].

$$D_{A,k} = \frac{2}{3} r_{ave} \sqrt{\frac{8RT}{\pi m_A}} \quad (13)$$

3.6.2 External Mass Transfer Limitations

A stagnant layer is created by the gas molecules around each catalyst pellet. Dependent of the gas flow velocity, the stagnant layer is limiting the diffusion of molecules through the layer into the catalyst. With a velocity high enough to ensure the same concentration at the catalyst surface and in the center of the gas flow, the external mass transfer is not a limiting factor for the reaction rate. [18]

The external mass transfer limitation in the gas phase around the catalyst can be described with the Carberry number in equation 14. The resistance due to mass transfer should be less than 5% in order to avoid significant falsification of the kinetic results. [17]

$$Ca = \frac{R_{V,A}^{obs}}{k_g a_v c_b} = \frac{c_b - c_s}{c_b} < \frac{0.05}{n} \quad (14)$$

As seen in equation 14, the external mass transfer is defined by the difference between the concentration in the gas and the concentration at the surface. The external mass transfer is through the gas film surrounding the catalyst particle [19].

3.7 Heat Transfer

The theory behind the heat transfer in the reactor tube is similar to the mass transfer. The external heat transfer is defined from the gas in the reactor to the catalyst surface and the internal heat transfer is defined inside the catalyst pores. The equations for the heat transfer limitations are described below.

3.7.1 Internal Heat Transfer Limitations

Heat transfer limitations can be caused by intraparticle temperature gradients. The internal heat transfer is suggested to be less than 10% and the expression is shown in equation 15. [17]

$$\frac{E_a}{RT_b} \left| \frac{-\Delta H_r D_{A,eff} c_s}{\lambda_{eff,p} T_b} \right| \left| \frac{R_{V,A}^{obs} (d_p/6)^2}{D_{A,eff} c_s} \right| < 0.1 \quad (15)$$

3.7.2 External Heat Transfer Limitations

The external heat transfer can be described by the expression in equation 16. It describes the heat transfer limitation in the surrounding gas around the catalyst; the gas film. [17]

$$\frac{E_a}{RT_b} \left| \frac{-\Delta H_r k_f c_b}{hT_b} \right| \frac{R_{V,A}^{obs}}{a' k_f c_b} < 0.05 \quad (16)$$

3.8 Power Law Kinetics

A forward gas phase reaction with A and B as reactants and C as a product can be described as in reaction 17.



To describe the reaction rate for reaction 17, a rate expression is needed. The rate expression is specific for each reaction and a rate expression is only describing one reaction in the reactor. One way to describe the reaction rate is by the power law equation. The general expression for the power law is described below in equation 18. [11]

$$r = k_n p_A^k p_B^l \quad (18)$$

Where n is the reaction number, A and B are the reactants, and k and l are the reaction order. The rate constant, k_n can be calculated with Arrhenius equation, shown in equation 19 [11].

$$k_n = k_{0,n} e^{\frac{-E_a}{R} \left(\frac{1}{T} - \frac{1}{T_{ref}} \right)} \quad (19)$$

The partial pressure used in the power law expression in equation 18 can be calculated from the molar fraction of the required component and the total gas pressure. The molar fraction in the gas phase in the reactor is used for this calculations. Equation 20 below shows how the partial pressure of a component i can be calculated [20].

$$p_i = z_{g,i} P_{g,tot} \quad (20)$$

3.8.1 Development of Intrinsic Kinetic Model

The kinetics used in this project have been developed beforehand by Iryna Bennett, Senior Process Engineer at Johnson Matthey. Based on Schmidt's [13] data she obtained the rate expressions for reaction 1 - 5 as well as regressed the kinetic parameters. The structure of the rate expressions are based on first guesses from literature and follows the power law as described in *3.8 Power Law Kinetics*. The

first guesses were further on fitted to experimental data to obtain the kinetic parameters. The first guesses for the rate expression for reaction 1 - 5 is shown below in equation 21 - 25. [13]

$$r_1 = k_1 p_{MeOH}^a p_{H_2O}^b \quad (21)$$

$$r_2 = k_2 p_{FA}^c \quad (22)$$

$$r_3 = k_{3,f} p_{MeOH}^d - k_{3,r} p_{DME}^e p_{H_2O}^f \quad (23)$$

$$r_4 = k_4 p_{DME}^g p_{H_2O}^h \quad (24)$$

$$r_5 = k_5 p_{MeOH}^i p_{FA}^j p_{H_2O}^k \quad (25)$$

Iryna Bennett obtained the kinetic expression for all five reactions. The complementing kinetic parameters; the frequency factor, the activation energy and the reaction order were regressed by Iryna Bennett as well.

The experimental data provided by Schmidt [13] was used by Iryna Bennett when performing the regression of the kinetic parameters. The experimental measurements were performed in a small-scale reactor set-up, with five smaller reactor tubes. The tubes have an inner diameter of 4 mm. For the kinetic measurement, the tubes were loaded with two layers, one inert layer of quartz sand followed by a mixed layer of catalyst. The catalyst was crushed and sieved to a grain size of 212-250 μ m. The inert had larger particle size and were used as the top layer to decrease the pressure drop along the tube. [13]

3.9 Deshmukh Kinetic Model

Another kinetic model which describes the reaction rates of the five main reactions taking place in the **FORMOX** reactor, is described in literature by Deshmukh [10]. The experimental study has been performed on a catalyst provided from Johnson Matthey Formox AB. The rate expressions below describe the rate of reaction 1 - 2. [10]

$$r_{FA} = k_{FA} \theta_{MeOH} \theta_{O_2} \quad (26)$$

$$r_{CO} = k_{CO} \theta_{FA} \theta_{O_2} \quad (27)$$

Reaction 3 is considered as an equilibrium reaction and the reaction rate is calculated differently compared to the reaction rates above in equation 26 and 27. The first term in equation 28 describes the forward reaction rate and the term to the right describes the reverse reaction rate. [10]

$$r_{DME} = k_{DME,f} P_{g,MeOH} - \frac{k_{DME,f}}{K_{DME}^{eq}} \frac{P_{g,DME} P_{g,H_2O}}{P_{g,MeOH}} \quad (28)$$

Equation 29 describes the kinetic expression for reaction 4 and has the same structure as equation 26 and 27.

$$r_{DME-FA} = k_{DME-FA} \theta_{DME} \theta_{O_2} \quad (29)$$

Reaction 5 is considered as an equilibrium reaction according to Deshmukh [10]. The rate expression in equation 30 is structured in the same way as for the equilibrium reaction 3 in equation 28.

$$r_{DMM} = k_{DMM,f} P_{g,FA} P_{g,MeOH} - \frac{k_{DMM,f}}{K_{DMM}^{eq}} \frac{P_{g,DMM} P_{g,H_2O}}{P_{g,MeOH}} \quad (30)$$

To calculate the value for the rate constants k_{FA} , k_{CO} , $k_{DME,f}$, k_{DME-FA} and k_{DMM} in equation 26 - 30, the Arrhenius equation in 31 was used.

$$k_n = k_{0,n} e^{\frac{-E_a}{RT}} \quad (31)$$

This Arrhenius equation is a simplified version of the Arrhenius equation in equation 19, since the expression is not based on a reference temperature. The regressed kinetic parameters to calculate the rate constant from the literature study and are shown in Table 1.

Table 1: Regressed parameters from experimental work performed by Deshmukh [10].

Parameter in Deshmukh	Definition	Value from Deshmukh
$k_{0,FA}$	Frequency factor for reaction 1	1.5e7 [mol kg ⁻¹ s ⁻¹]
$k_{0,CO}$	Frequency factor for reaction 2	3.5e2 [mol kg ⁻¹ atm ⁻¹ s ⁻¹]
$k_{0,DME,f}$	Frequency factor for reaction 3	1.9e5 [mol kg ⁻¹ atm ⁻¹ s ⁻¹]
$k_{0,DME-FA}$	Frequency factor for reaction 4	6.13e5 [mol kg ⁻¹ s ⁻¹]
$k_{0,DMM,f}$	Frequency factor for reaction 5	4.26e-6 [mol kg ⁻¹ atm ⁻² s ⁻¹]
E_{FA}	Activation energy for reaction 1	86.00 [kJ mol ⁻¹]
E_{CO}	Activation energy for reaction 2	46.00 [kJ mol ⁻¹]
$E_{DME,f}$	Activation energy for reaction 3	77.00 [kJ mol ⁻¹]
E_{DME-FA}	Activation energy for reaction 4	98.73 [kJ mol ⁻¹]
$E_{DMM,f}$	Activation energy for reaction 5	46.50 [kJ mol ⁻¹]

In the equations 26-30 above, θ is defined as the surface fraction of each component at the catalyst surface. The rate expressions above are dependent of the surface fraction of methanol, oxygen, formaldehyde and *DME*. The equation for the surface fractions for these respective components are shown in equation 32-35. [10].

$$\theta_{MeOH} = \frac{K_{MeOH}P_{g,MeOH}}{1 + K_{MeOH}P_{g,MeOH} + K_{H_2O}P_{g,H_2O}} \quad (32)$$

$$\theta_{O_2} = \frac{K_{O_2}P_{g,O_2}^{1/2}}{1 + K_{O_2}P_{g,O_2}^{1/2}} \quad (33)$$

$$\theta_{FA} = \frac{P_{g,FA}}{1 + K_{MeOH}P_{g,MeOH} + K_{H_2O}P_{g,H_2O}} \quad (34)$$

$$\theta_{DME} = \frac{K_{DME}P_{g,DME}}{1 + K_{DME}P_{g,DME}} \quad (35)$$

The adsorption constants K_{MeOH} , K_{O_2} , K_{FA} and K_{DME} in the surface fraction expression were calculated with the Arrhenius equation 19. The kinetic parameters, the pre-exponential constants and the activation energies, was given in the literature study and are shown in Table 2.

Table 2: Adsorption constants and activation energies regressed by Deshmukh [10].

Parameter in Deshmukh	Definition	Value from Deshmukh
$K_{0,MeOH}$	Pre-exponential factor for $MeOH$	2.6e-4 [atm^{-1}]
K_{0,O_2}	Pre-exponential factor for O_2	1.423e-5 [$atm^{-1/2}$]
K_{0,H_2O}	Pre-exponential factor for H_2O	5.5e-7 [atm^{-1}]
$K_{0,DME}$	Pre-exponential factor for DME	5.0e-7 [atm^{-1}]
$E_{a,MeOH}$	Activation energy for $MeOH$	-56.78 [$kJmol^{-1}$]
E_{a,O_2}	Activation energy for O_2	-60.32 [$kJmol^{-1}$]
E_{a,H_2O}	Activation energy for H_2O	-86.45 [$kJmol^{-1}$]
$E_{a,DME}$	Activation energy for DME	-96.72 [$kJmol^{-1}$]

In the literature paper, reaction 3 and 5 is considered as equilibrium reactions. The equilibrium constants has to be calculated for DME and DMM respectively according to the equations shown in 36 and 37 [10].

$$K_{DME}^{eq} = \left[\frac{P_{g,DME}P_{g,H_2O}}{P_{g,MeOH}^2} \right]_{eq} \quad (36)$$

$$K_{DMM}^{eq} = \left[\frac{P_{g,DMM}P_{g,H_2O}}{P_{g,MeOH}P_{g,FA}} \right]_{eq} \quad (37)$$

The regressed parameters for the equilibrium constant from Deshmukh [10] are shown in Table 3. These values were used in the rate expressions 26-30 when implementing the equations and parameters into the reactor model.

Table 3: Equilibrium constant regressed by Deshmukh [10].

Parameter in Deshmukh	Definition	Value from Deshmukh
K_{DME}^{eq}	Equilibrium constant DME in reaction 3	$exp(-2.2158 + 2606.8/T)$
K_{DMM}^{eq}	Equilibrium constant DME in reaction 5	$exp(-20.416 + 9346.8/T)$

The developed kinetics above are validated for 230-260°C according to the literature paper [10].

3.10 Pilot Plant Reactor

To validate the reactor model, a validation was made against a pilot reactor. Measured pilot plant data were required from the real reactor in order to evaluate how well the reactor model described it. The data used in this project was collected by Johnson Matthey Formox’s R&D team and the experiments was performed on their pilot reactor in the laboratory.



Figure 10: Picture of the pilot reactor in the pilot hall at Johnson Matthey in Perstorp [21].

The data used for the validation against the pilot reactor was collected from the reactor tube on the right side in Figure 10. The pilot reactor corresponds to a full-

scale reactor with only one reactor tube. Along the tube, numerous thermocouples are placed in the middle of the tube to obtain specific measurements at different heights. The thermocouples are placed at a certain height, measured from the top of the tube. Due to the installed thermocouples, it is possible to evaluate how the temperature and composition behave along the tube at the different catalyst layers.

4 Method

An intrinsic kinetic model includes neither mass nor heat transfer limitations, it only considers the bulk flow to the catalyst surface. When a model is further developed to an apparent model, it includes the material transport inside the catalyst pores [11]. First only the kinetic model was used in ACM, aimed to describe the the intrinsic reactor model. After that, an apparent model was used for the reactor model. A 2D reactor model was used where mass and heat transfer occurred in the radial direction through diffusion and described the different molar flows in the middle of the tube and at the wall.

It was assumed that reaction 1 - 5 was the main reactions in the tube. Reaction 6 and 7 was neglected when modeling the reactor since they are considered as minor side reaction and are assumed not to affect the other reactions significantly [10].

The design of the reactor model was carried out in an earlier project inside Johnson Matthey, described in *2.5 Existing Reactor Model*. This model was using pseudo kinetics as a placeholder until the kinetics model was to be developed. In this master thesis project, a kinetics model was implemented into the existing reactor model. The improved reactor model was further on validated against the pilot reactor. Since the development of the kinetics also was an ongoing project inside the company, the kinetic model used in the reactor model was changed and modified a couple of times.

4.1 Modeling Set Up

The modeling work was performed in Aspen Custom Modeler - Version 10, described in *2.4 Aspen Custom Modeler*. In order to compile the code, a Fortran G95 compiler was installed in the computer as well. The procedure were coded separately and then used in the main code. When any new code was added to any procedure, the procedure was compiled and the code was generated. When the code was generated the folder where the file was saved was updated and the main code was reading the new procedures when running the model.

Aspen version 10 was used in combination with Fortran Compiler G95 to be able to run the code. The code was compiled within the fortran compiler and created a library from where the model could be run. It was evaluated if Aspen Version 11 could be used, but the fortran compiler generates a 32-bits code and a newer version of Aspen Plus could only accept 64-bits. It was concluded that Aspen version 11 could not be used together with the fortran compiler G95.

4.1.1 Troubleshooting

When implementing any code to ACM, the changes were small and the program was compiled and ran after every change. Some of the errors occurred was shown in the simulation message window in Aspen when the model was compiled was in this case easy to detect. If no errors were shown in the simulation window, but the code was not generated correctly, it was also possible to troubleshoot with a program called command prompt window. This was a built-in program in the Windows package and was used outside Aspen, in the folder environment. It was then possible to run the procedure through the command prompt window and if any errors occurred while running, they were shown in the command prompt window.

When any problem occurred to the main model, it was more difficult to detect it. It was not possible to run the main code through the command prompt window and there was no debug function observed in Aspen Custom Modeler.

4.1.2 Running Mode

When running the code, it was possible to run in different modes. In this project initialization and steady state mode was used. The initialization was going through the code and solving the algebraic equations, and the code had to be initialized before running in steady state. Another option to initialize was through snapshots. When running a code in steady state mode with successful convergence, it was possible to save a snapshot. When further on applying small changes to the code it was possible to use the values from the previous snapshot as initial guesses. When running the model in steady state, the model was trying to solve all the partial differential equations implemented in the code. [7]

4.1.3 Obtained Results

After running the code, both in initialization and steady state mode, the result could be received. The results were found under a tab called *Flowsheet*. The parameters calculated in main code was shown as output parameters and defined as the result. It was possible to obtain the result of the calculated parameters from the procedure as well. To do so it was necessary to code the wanted parameter as an output parameter from the procedure and call it in the main code.

4.2 Verification of Calculation Method

To make sure the correct calculation method of the reaction rates was implemented into the code, a primary verification was made in Excel to minimize the risk of errors implemented in the code. The reaction rates were calculated according to equation 21-25. The regressed kinetic parameters from Iryna Bennett, such as the rate constants k_1 , k_2 , k_3 , k_4 , k_5 and the exponents a-h, were used when calculating the reaction rates. The partial pressures were calculated according equation 20 and used in the rate expressions. The reaction rate was recalculated to the formation rate to compare to the experimental data from Schmidt [13].

To determine the formation rate of each component, the calculated reaction rate and the stoichiometric coefficient in every reaction was considered. The equation to calculate the formation rate for component i is shown below in equation 38 [20].

$$s_i = \nu_{i,r1}r_1 + \nu_{i,r2}r_2 + \nu_{i,r3}r_3 + \nu_{i,r4}r_4 + \nu_{i,r5}r_5 \quad (38)$$

After calculating the formation rate in Excel, the values were compared with the values from Schmidt's [13] experimental work. The measured values represented the formation rate for all the compounds leaving the reactor.

4.3 Implementation of Kinetic Model

A separate kinetic model was made in the beginning including only the procedure with the rate expressions. A simplified main model was created to test the kinetic model separately. This was done to make sure the kinetic model was performing well before implementing it to the existing model. The reactor model described in *2.5 Reactor Model* has a high complexity and the kinetic model is also quite complex. The implementation of the procedure to the reactor model could easily cause some difficulties.

4.3.1 Implementation of Power Law

When implementing the kinetic model, the procedure from the reactor model was used. The main structure was already implemented but the rate expressions were pseudo kinetics, working as placeholders. The original reactor model included only 3 reactions and 8 components.

The majority of the equations in the procedure was replaced with the new kinetic equations and parameters. The new kinetic expressions were implemented in the procedure for the reaction rates and the regressed parameters and the stoichiometric for the reactions were defined in the function as well. The regressed parameters implemented were the rate constants, the activation energy for each reaction, and the reaction order. The code was compiled when something new was added to make sure it compiled properly.

Since the original code only considered 3 reactions and 8 components, the additional reactions and compounds had to be defined as well. *DMM* was added as a compound in the main code and also in the procedures where the reaction rates were defined. Reaction 4 and 5 were added as reactions since they were not included in the first version of the code and they were also added in the main code as well as in the procedure with the rate expressions.

When the test model was completed, with the kinetic procedure and the simplified main code, the code was run. The output result for the formation rate was compared to the calculated result in *4.2 Verification of Calculation Method* to compare if the same results were obtain with ACM.

4.4 Parameters

Before implementing the kinetic model into the reactor model, some parameters had to be modified in the reactor model to be able to represent the pilot plant data. Some of these parameters will be described below.

It was of high importance that all physical properties were correct and matched with the properties for the pilot plant reactor. In this section, some of the important properties are highlighted and it is described how they were obtained and used in the reactor model.

4.4.1 Inlet Composition

The inlet composition was given in NI/min which stands for normal liters per minute, at 1 atm and 0°C. The total inlet flow was calculated by the sum of each component flow and the molar fraction is calculated as seen in equation 39 [20].

$$x_i = \frac{n_i}{n_{tot}} \quad (39)$$

4.4.2 Tube Density

The tube density, also known as the packed bed density, was calculated before implemented into the code. To calculate the tube density the following equation was used. [22]

$$\rho_{tube} = \frac{m_{pellet}}{V_{pellet}} \quad (40)$$

The weight of the pellet was measured for the different layers in the tube and the volume was calculated based on the dimensions of the pellet.

4.4.3 Bed Geometric Surface Area

The bed geometric surface area (GSA) had to be implemented into the code as well to describe the catalyst load. To calculate the GSA, equation 41 was used. [23]

$$GSA = \frac{V_{pellet}}{m_{pellet}} \rho_{tube} \quad (41)$$

4.4.4 Inlet Composition

When implementing the inlet composition into the reactor model, the average gas concentration was used. To obtain the average molar fraction for each compound, equation 42 was used. [25]

$$x_{i,ave} = \frac{x_{i,in} - x_{i,out}}{2} \quad (42)$$

The average molar fraction was calculated in Excel before implementing it into the reactor model. The calculations in the Excel sheet was coupled to easy recalculate the value when comparing to another data point.

4.5 Implementation to Reactor Model

When the test model was working and running with no errors, the procedure was implemented into the existing reactor model. In the same way as in 4.3.1 *Implementation of Power Law*, *DMM* had to be added as well as reaction 4 and 5. Some of the existing procedures were adjusted with the new compound *DMM*, the ones calculating the enthalpy and the molecular weight and the molecular weight of *DMM* and the coefficient for the enthalpy calculations was added as well. The main model was modified with *DMM* and reaction 4 and 5 was also modified to use the new procedure including the kinetics. To connect the procedure to the main code a call line was used, defined with the requested outputs and the required input parameters.

When the model was running properly, the kinetics were verified again. To verify the implementation, the values used in the Excel calculations was defined in Aspen, such as the temperature, pressure and composition. If the Aspen model provided the same results as when calculating it in Excel, it was an indication that the kinetics model was implemented in the correct way.

4.6 Implementation of Heat and Mass Transfer Limitations

External mass and heat transfer limitation were already included in the reactor model. After finalizing the implementation of the kinetics model, this project aimed to implement the internal mass and heat transfer as well. In the reactor model, the mass and heat transfer, was be described in the axial and radial direction.

In order to implement the internal mass and heat transfer limitations, the catalyst pellet had to be modeled. The catalyst is a ring shaped, hollow pellet. If the condition in equation 43 was fulfilled, the geometry of the pellet could be considered as a slab. When calculating the ratio for the catalyst used in this project, the value was a bit below 0.9. [25]

$$\frac{r_{inner}}{r_{outer}} > 0.9 \quad (43)$$

In order to describe the external and internal mass and heat transfer limitations, the equation are to be combined in the reactor model to obtain the global mass and heat transfer expression.

4.7 Validation Against Pilot Plant

When the reactor model was completed regarding the implementation of the kinetic model, it was validated against the pilot reactor. The input parameters were ad-

justed in order to match the pilot reactor, and the simulated results were compared with the measured data from the pilot reactor.

4.7.1 Input Parameters from Pilot Reactor

In order to validate the reactor model against the pilot reactor, the same input parameters from the pilot plant had to be implemented into the code. The operating conditions and inlet compositions had to be the same as for the experimental performance at the pilot plant. The parameters from the pilot reactor, implemented into the reactor model, is shown below in Table 4.

Table 4: Input parameters to validate against the pilot reactor.

Reactor Parameters	Bed Parameters	Operation Parameters	Inlet Composition
L_{tube}	GSA	T_{in}	$x_{MeOH,in}$
$D_{i,tube}$	ρ_{bed}	$T_{coolant}$	$x_{H_2O,in}$
$D_{o,tube}$	k_s	P_{in}	$x_{O_2,in}$
		P_{out}	$x_{N_2,in}$
			$\dot{n}_{tot,in}$

The parameters describing the pilot reactor, such as the inlet composition, temperatures and pressures, are measured from the pilot reactor, by the R&D team at Johnson Matthey.

4.7.2 Different Layers of Catalyst

The different layers of catalyst in the reactor tube, the loading plan, had to be modeled. In ACM, the height of the catalyst was considered as the full length, excluding the pure inert layers. The length of the tube in the main code was divided into sections with specific catalyst properties in each layer. The bed geometric surface area as well as the tube density, was calculated for each layer and implemented to its corresponding layer in the code.

The tube density and the bed geometric surface area were calculated for each layer according to equation 40 and equation 41, using the catalyst properties for the corresponding layer. It was assumed that the same kinetic model could be used for the different layers.

5 Result and Discussion

In this section the results of the implementation of the kinetic model will be described. In an early stage of the project, some errors were obtained with the kinetic model and had to be improved. The development of the kinetic model will be described as well and was a big part of the project going forward. An evaluation and

discussion of the reactor model is also included in this section where the reactor model was validated against the pilot reactor.

5.1 Development and Implementation of Kinetic Models

This section describes the different versions of the kinetic models and how they were tested in the simplified model before implemented into the reactor model.

The Excel calculation described in *4.2 Verification of Calculation Method* was adjusted when a new kinetic model were developed. The calculations in Excel was used to verify that the correct method was used to determine the reaction rate and it was also used for comparison to the Aspen reactor model later on, to make sure the code was implemented correctly.

5.1.1 Power Law

Version 1: Kinetic model developed by Iryna Bennett and is described by the power law. The kinetic parameters are regressed with gauge pressure.

The power law kinetics is used in the kinetic model described in the method. *Version 1* was implemented into the reactor model as described in *4.5 Implementation to Reactor Model*. The implementation was successful and the model compiled and ran correctly.

When the model was implemented and run in Aspen, two errors were found in *Version 1*. The kinetics developed by Iryna Bennett was evaluated by Robert Gallen and the following problems were identified.

- Stoichiometric factor for DME in reaction 5.
- The use of gauge pressure.

5.1.2 Refitted Power Law

Version 2: Kinetic model developed by Robert Gallen, based on Version 1 with the power law expression. The kinetic parameters are refitted and the regression was made with absolute pressure.

A refit of the model was performed by Robert Gallen where new kinetic parameters were regressed [25]. Since the kinetics was being improved continuously in an

ongoing project, the reactor model used the latest kinetics throughout the whole project.

When the new kinetic parameters were regressed by Robert Gallen for the power law expression, it was implemented in the kinetic model. Since the structure of the rate expressions was similar to the one in *Version 1*, it was just to change the refitted parameters in the model. The output parameters were compared to the reaction rates from the Schmidt's [13] experimental data to make sure the kinetic model was implemented correctly. A comparison between the model from ACM and the experimental data, was made by a parity plot and the plot can be seen in Figure 11, where the reaction rates are calculated.

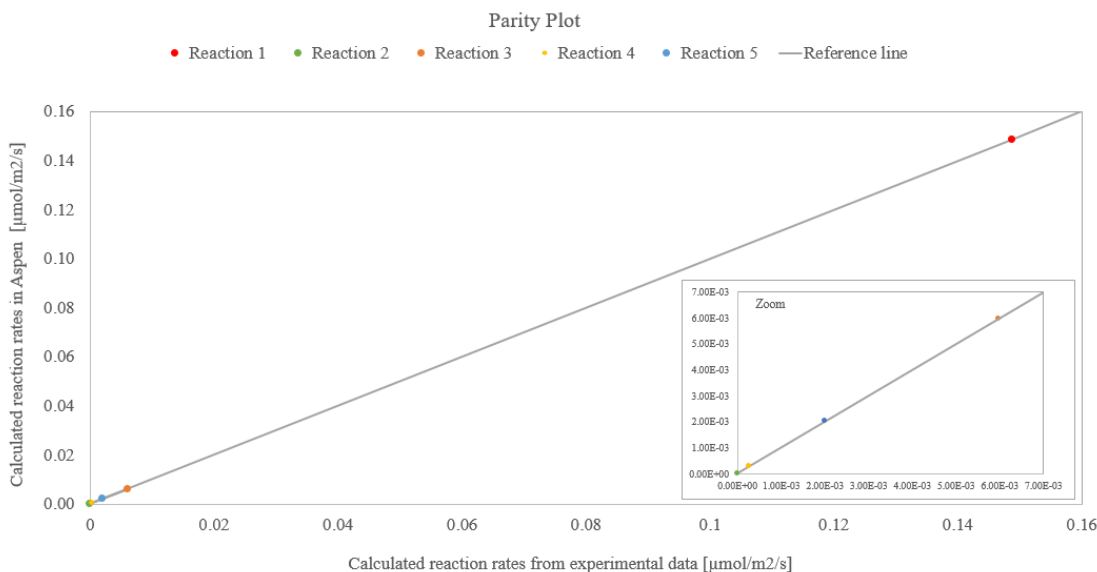


Figure 11: Comparison of reaction rate between experimental data and calculated values in the kinetic model.

As seen in Figure 11, the reaction rate calculated by the kinetic model in Aspen was almost the same as the experimental data. An almost identical result indicates that the model was successfully implemented.

When further changing the inlet composition to the values from the pilot plant, some numerical errors occurred. It was the inlet molar fraction of H_2O causing the problem. When the molar fraction was 0 and its exponent was negative, the model was not running, since this is an undefined mathematical expression. When the kinetics test was performed this error was avoided, the only components with inlet composition set to 0 in the main code was H_2 and CO . H_2 and CO do not affect the rate expressions since there are no partial pressure of neither H_2 nor CO in equation 21 - 25. The problem occurred when the inlet composition of H_2O was set to 0.

It cannot be guaranteed that the concentration is nonzero for the dependent components $MeOH$, H_2O , O_2 , FA and DME along the whole tube. The kinetic

model had to be improved to be able to run the reactor model and compare with the pilot plant data.

The model was not able to run properly and could not be compared to the pilot reactor until the new kinetics model was developed. It was assumed that the new kinetics would change its structure from power law and behave more like the kinetics described by Deshmukh [10]. Meanwhile when the kinetics was under development, the kinetics model from literature was used [10]. Since the new kinetic model was assumed to look like the one Deshmukh [10] is describing, it was time saving to change to this model meanwhile.

5.1.3 Deshmukh Kinetic Model

Version 3: Deshmukh kinetic model from literature [10].

The power law kinetics were giving numerical errors, when the model was running with no inlet water. The partial pressure of water was zero with an associated negative exponent. A kinetic model from literature was used instead and is called *Version 3* in this project.

When changing the kinetic model into the one from literature, several changes had to be made in the procedure with the rate expressions. Since the rate expressions from Deshmukh [10] was different in many ways from the power law expression, the equations had to be adjusted and replaced with the new kinetic model. All the new parameters had to be defined and implemented in the procedure as well. The separate kinetic model was run by itself and the results for the reaction rates were compared with the graphs in the paper. The comparison between the result in Aspen and the value in the graphs was to validate the implementation of the kinetic model. When comparing with the reaction rates from the graphs in the paper, the inlet composition and temperature were changed according to the inputs from the literature [10].

When running this kinetics model, the same conditions as in the literature paper were implemented in the code. The inlet composition varies depending on which reaction expression was evaluated. The parameters used for evaluating reaction 1 can be seen in Table 5

Table 5: Operation condition used when running Deshmukh kinetics [10].

Parameter	Value
P_g	1 atm
T_g	230°C
z_{g,N_2}	0.85
z_{g,O_2}	0.05
$z_{g,MeOH}$	0.1

The Deshmukh paper [10] defines their reactant conversion to be between 5-10%, but the exact number cannot be found in the paper. A 10% reactant conversion was assumed when determine the inlet flow with the values from the table above, and equation 42 is used to calculated the average molar fraction.

To compare with the result from the graphs in the paper, an online tool was used to extrapolate the values for a more reliable comparison [26]. To validate if the code was implemented correctly and to evaluate how the kinetics model behaved, the output from Aspen was compared with the result from the literature paper. For reaction 1 and 2, the reaction rates from the model was almost twice as big compared to the graphs in the paper. In the following figures the results from Aspen were compared with the literature data. A methanol conversion of 10% were assumed when the inlet compositions were implemented in the code. The implementation and operation conditions are described above. The difference between the two graphs below is the temperature, where Figure 12 is operating at a temperature of 230°C and Figure 13 is operating at a temperature of 260°C. The blue dots in figures shows the results of the reaction rate from the literature paper and the red dots in the graphs are results from the reactor model divided by 2. [10]

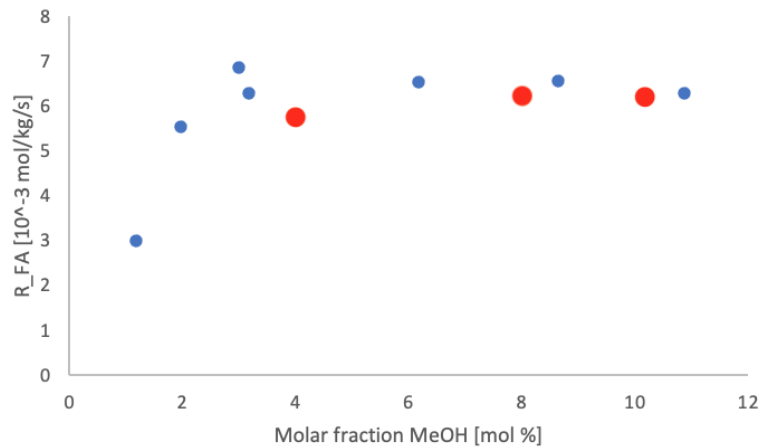


Figure 12: Comparison of reaction rate between results from Deshmukh [10] and ACM to validate the kinetic model. The red dots shows the result from the Aspen model and the blue dots represents the reaction rate from Deshmukh [10]. The reaction rates were calculated at a temperature of 230°C, inspired by Deshmukh [10].

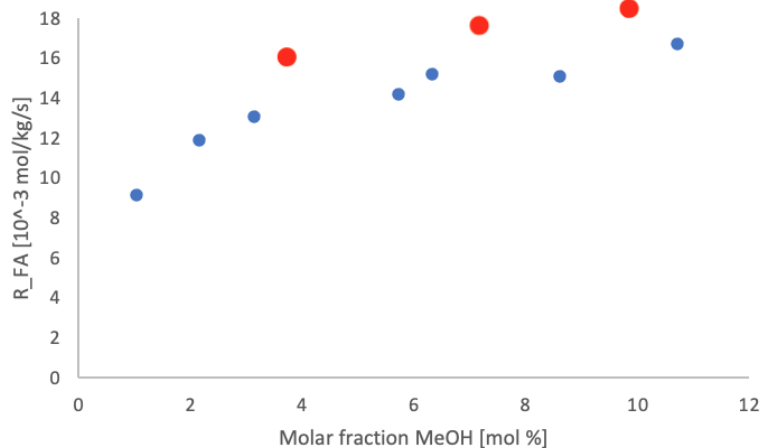
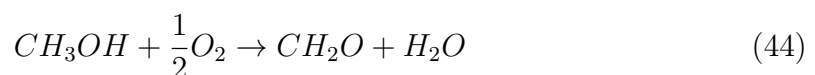


Figure 13: Comparison of reaction rate between results from Deshmukh [10] and ACM to validate the kinetic model. The red dots shows the result from the Aspen model and the blue dots represents the reaction rate from Deshmukh [10]. The reaction rates were calculated at a temperature of 260°C, inspired by Deshmukh [10].

The results of the reaction rates from Aspen fits the results from Deshmukh [10] when divided by 2. A possible reason why the result was off by a factor of 2 could be explained by the stoichiometric coefficients. The reactions are defined in the paper as a seen in equation 44.



It is common to use stoichiometric coefficient without decimals, and therefore multiply every stoichiometric coefficient by 2 to avoid this. A possible explanation is that Deshmukh [10] used this way, to multiply by 2, when defining the stoichiometric coefficients in the calculation for the reaction rates. When providing the results, the reaction rate has to be divided by 2 again to receive the correct value.

The reason why the results were off by a factor of 2 was difficult to evaluate. This problem was discussed internally at Johnson Matthey and the final possible explanation was the use of stoichiometric coefficients. When new kinetic parameters sets will be developed internally at Johnson Matthey, this factor will not affect the result anymore, since it will be known what procedure was used when regressing the parameters.

5.1.4 Rebased and Refitted Kinetic Model

Version 4: Based on the Deshmukh kinetics model from literature [10], two kinetic model were developed: a) The kinetic model was rebased including a reference temperature b) The rebased kinetic model was refitted to the experimental data from Schmidt [13].

To improve the kinetic model from literature [10], the model was rebased. *Version 3* did not consider a reference temperature in the rate equations. A rebased expression includes a reference temperature when calculating the Arrhenius expression, as shown in equation 19. The reference temperature contributes with a numerical stability to the expressions. The data from Deshmukh [10] was used to rebase the expression and to determine the reference temperature. A new parameter set was developed with the results from Deshmukh [10], now with an expression including the reference temperature. This work was done by Robert Gallen.

The new kinetic model including the reference temperature, was also refitted to experimental data from Schmidt [13] to describe the pilot reactor. This new refit provided an entire new set of kinetic parameters.

In total, three sets of kinetic parameters was obtained using the structure of Deshmukh kinetic model - the original one from the paper [10], the rebased expression based on the results from the paper and the rebased expression refitted to the data from Schmidt [13]. All the three models were implemented individually into the reactor model to evaluate the difference between the parameter sets.

When implementing the two models in *Version 4*, the Arrhenius equation was adjusted and the reference temperature was added. The rest of the equations coded in the reactor model could be kept as they were, and only the new values for the kinetics parameters were implemented into the code.

5.2 Reactor Model

The complexity of the reactor model increased when including *Version 3* or *Version 4*, since several new equations were added.

5.2.1 Convergence Problem in Steady State

When the kinetic models in *Version 4* was implemented and combined with the reactor model, the simulation was not able to converge when running in steady state. The separate kinetic model was converging when running in steady state and the reactor model without the kinetics implemented was also converging at steady state. This indicated a problem when combining the reactor model with the kinetics model, since the complexity of the entire model increased a lot. When ACM tries to converge, it is aiming to minimize the error. The error was showed when running and it was a high number when the model faced a convergence problem. The number of iterations reached 1000 before the run was stopped. It was possible to rerun in steady state and the error decreased every time. When reaching an error around 10^{-3} , it was not possible to run the model and the message - steady state solution failure - occurred.

It was investigated if the equilibrium equations effected the convergence of the model. Since the denominator in equation 28 and 30 included the partial pressure of methanol, there was a risk of dividing by 0 if the composition of methanol went down to 0, and this could encounter a numerical error. The reaction rate expression for reaction 3 and 5 was removed from the code to see the effect. The problem to converge was the same with and without equation 28 and 30 and the same simulation message was obtained in both cases.

Another try to solve the problem was to increase the tolerance and to decrease the number of points in the axial and radial direction. Although, the same steady state solution failure appeared.

Another test was made, a factor 10^{-7} was added to the reaction rate in the procedure. It was implemented as seen below in equation 45. The r in the code represents an array with all the reaction rates and the factor was automatically considered for all the reaction rates.

$$r = 10^{-7} \cdot r \quad (45)$$

In this way the value from the procedure would not affect the main code to much. Aspen Custom Modeler was not a robust program and it did not accept big changes in the code. When running in steady state with the modified reaction rate result, the model converged. The factor was increased with small changes and a snapshot from previously run was used as an initial guess, as described in *4.1.2 Running Mode*. Due to the small changes it was possible to decrease the factor down to 10^{-3} . The procedure calculated a reaction rate with the unit $\frac{mol}{m^2s}$ whereas the main code considered the reaction rate with a unit of $\frac{kmol}{m^2s}$. The factor 10^{-3} was

multiplied with the reaction rate in the procedure and the code was converging in steady state.

The code was converging and running in steady state, but when analysing the results, no reaction was taking place. The code had been forced to converged, when the tolerance was decreased and it was not running properly. It was also observed that the pressure was not following the expected profile and the bed pressure gradient coefficient had to adjusted. The tolerance was decreased again and with only two reaction rate expressions included, the factor 10^{-7} was implemented and decreased until it reached 10^{-3} . With decreased tolerance and adjusted bed pressure gradient, the model was converging and giving expected results. This method was possible to apply on *Version 4 - a*. *Version 4 - b*, the refitted model, was not able to converge and due to the time limit of this project, the problem could not be solved.

5.2.2 Validation of Rebased Model Against Pilot Plant

The results from *Version 4 - a*, are presented in this section. The input parameters to ACM matched the pilot plant data in order to validate the output results from the model with the pilot reactor. Since the kinetic model from Deshmukh [10] was based on experimental data performed with a catalyst produced at Johnson Matthey in Perstorp, the kinetic parameters might be close enough to obtain a good result when validating against the pilot reactor.

Figure 14 shows the results for the outlet composition of the main components, the reactants and products included in reaction 1. The calculated deviation is shown in Table 6.

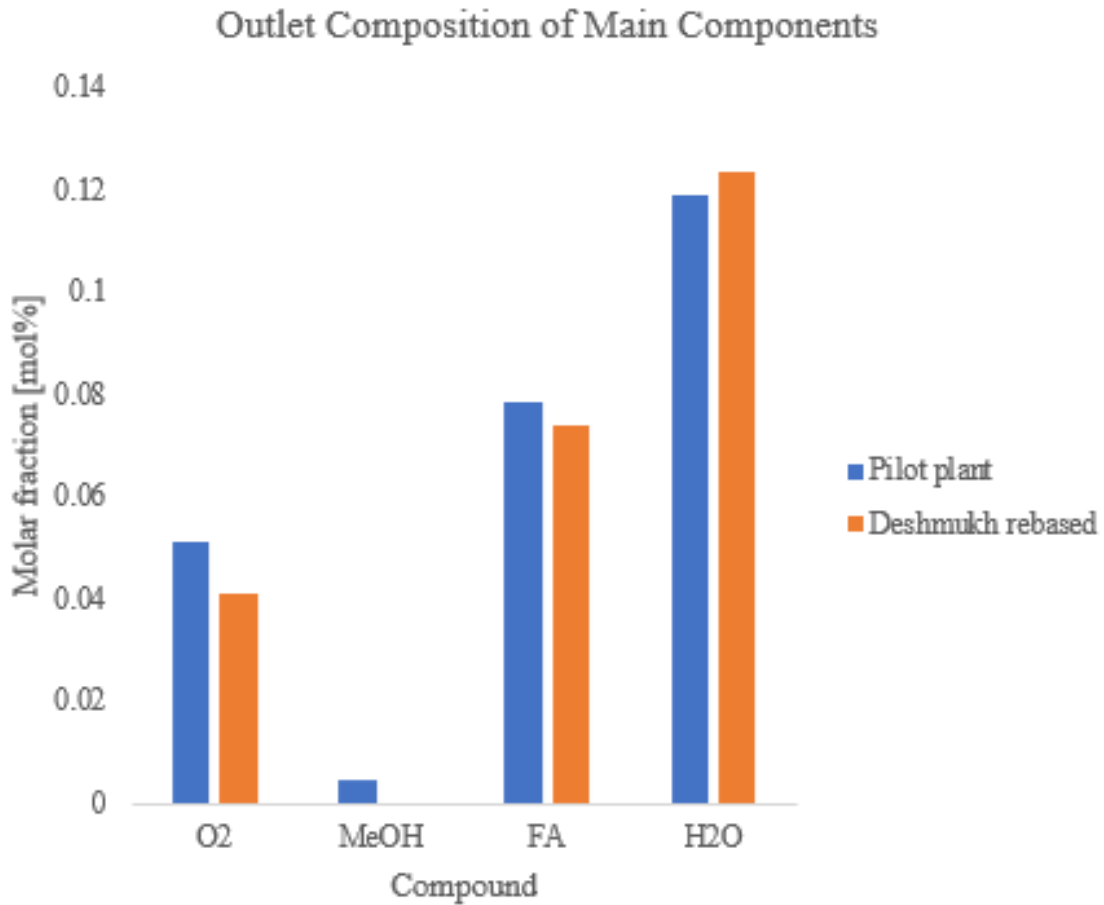


Figure 14: Validation against pilot reactor of the outlet composition of the main components.

Table 6: Calculated deviation of the outlet composition for the main components.

Compound	Relative Deviation Compared to Pilot Plant Data [%]
<i>O₂</i>	-19
<i>MeOH</i>	-95
<i>FA</i>	-5.6
<i>H₂O</i>	+3.6

As the figure above shows, the rebased model matches the outlet composition from the pilot plant data well, with relative deviation between +3.6% for water to -95% for methanol. The data from the pilot plant are the molar fraction measured in the outlet flow at the bottom of the tube and are not only considering reaction 1. According to the reactor model, more methanol and oxygen has been consumed compared with the expected values from the pilot plant. As seen in Table 6, the relative deviation for methanol is -95% and almost all the methanol is consumed.

Reaction 1 is the main reaction and the majority of the methanol and oxygen are used for this reaction to produce formaldehyde and water. As seen in Figure 14, the result from the rebased model shows that more water is produced than the pilot plant reactor shows. Although, less formaldehyde is produced than expected.

In Figure 15, the outlet composition for the produced side products are plotted. The calculated outlet composition are compared with the measured composition from the pilot reactor. The calculated deviation is shown in Table 7.

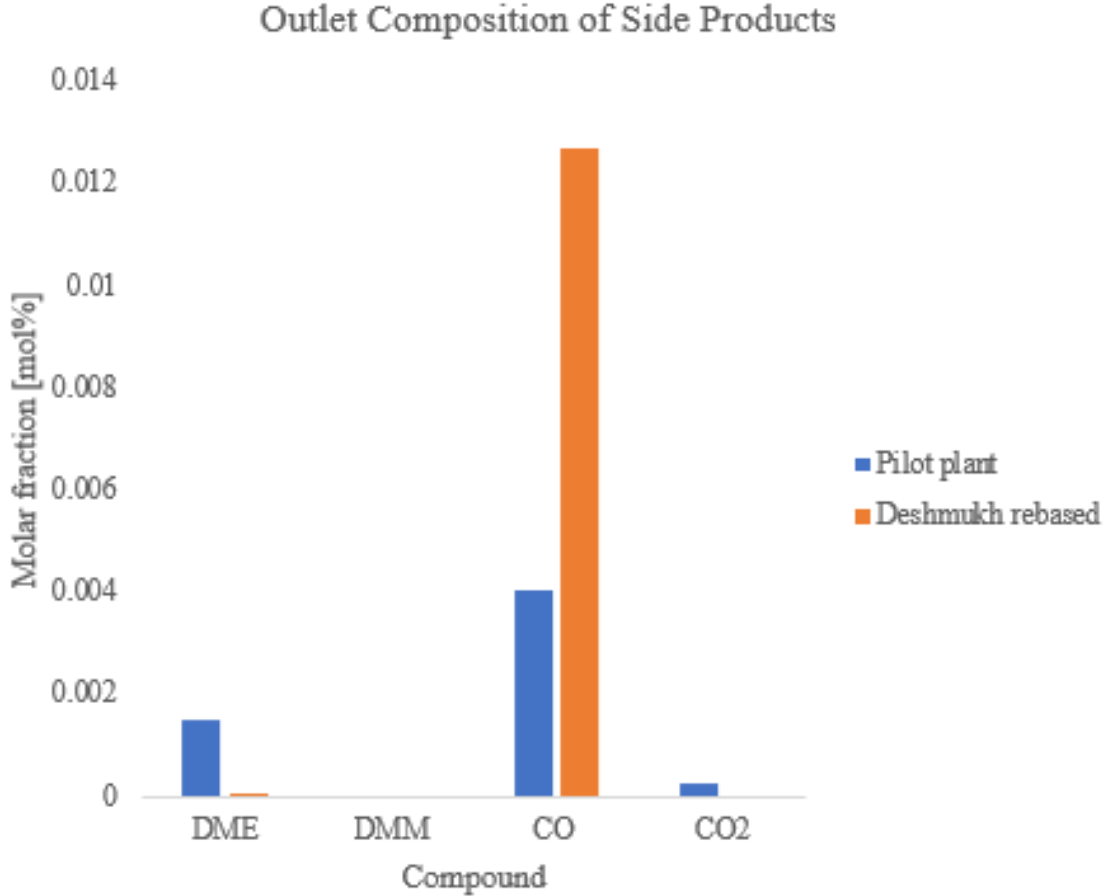


Figure 15: Validation against pilot reactor of the outlet composition of the side products.

Table 7: Calculated deviation of the outlet composition for the side products.

Compound	Relative Deviation Compared to Pilot Plant Data [%]
<i>DME</i>	-99
<i>DMM</i>	0
<i>CO</i>	+212
<i>CO₂</i>	-100

The outlet composition for the by products are not matching the values from the pilot plant data. The results in Figure 15 shows that no *DME*, *DMM* nor *CO₂* are produced in the simulation from the reactor model. *DMM* was expected to be 0 and the equation for the reaction rate *CO₂* are not included in the kinetics. Although, the result for the outlet composition of *DME*, indicates that the reaction rate for reaction 3 is lower than expected. *DME* is produced by *MeOH*, and since all the methanol was consumed in reaction 1, as seen in Figure 14, the reaction rate for reaction 3 will be decreased. The biggest difference seen in the figure above, is the production of *CO*. The reactor model produced more *CO* then the pilot plant, with a relative deviation of +212%. This result strongly indicated that the reaction rate for reaction 2 in the reactor model is higher than it should be since *CO* only is produced in reaction 2.

In Figure 16, the temperature profile along the tube is presented for the calculated values in the reactor model as well as the pilot plant temperatures. The simulation starts where the catalyst bed starts and the height on the x-axis, correlates to the top of the catalyst bed. When the temperature profile was measured for the pilot plant, the temperature was measured with thermocouples in the middle of the reactor tube. The temperature from ACM presented below was taken from the results in the middle of the tube to compare with the same profile as from the pilot plant.

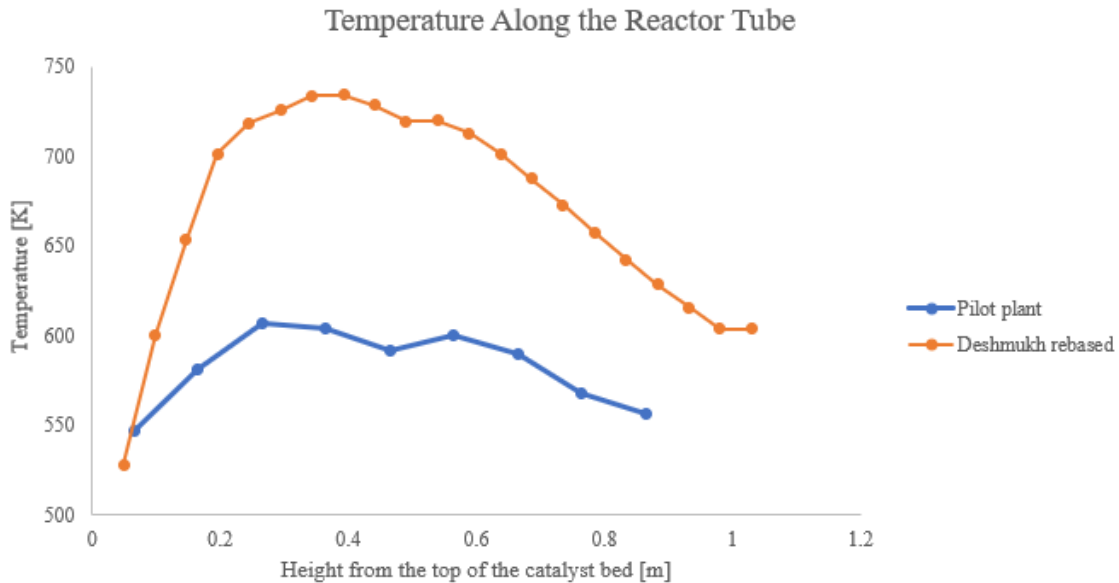


Figure 16: Validation against pilot reactor of the temperature profile.

The rebased model obtained a similar shape as the pilot plant, with two hot spots, as seen in Figure 16. The difference in temperature is quite high with a relative deviation of +15%, the model reaches a higher temperature compared to the pilot reactor. The reactions are exothermic in the reactor, the higher temperature could be explained by more heat released in the modeled reactor. The higher temperature achieved in ACM could also be explained by the heat transfer through the reactor

wall. The heat transfer fluid surrounding the reactor tube aims to cool the gas fluid inside the tube. If the heat transfer resistance is too high, the cooling effect is decreased and a higher temperature is reached in the reactor.

A possible explanation to the results in Figure 14 and 15, is a higher reaction rate of reaction 1 and reaction 2. Less formaldehyde was present in the outlet than expected and the reaction rate for reaction 2 was higher than it should, indicated by the high molar fraction of CO in Figure 15. CO is produced by formaldehyde, and by a higher reaction rate of reaction 2, decreases the outlet composition of formaldehyde. The reaction heat is calculated in the reactor model and the result shows that reaction 1 and 2 release more heat than the other reactions. A higher reaction rate of reaction 1 and 2 would explain the higher temperature obtained in Figure 16.

As discussed in *5.1.3 Deshmukh Kinetic Model, Version 3* was giving a result with a deviation of the factor 2 between the Aspen model and the literature result for reaction 1 and 2. The higher reaction rates for reaction 1 and 2, observed in this section, could be explained by this factor. It is difficult to evaluate what the deviation from literature depends on but a possible explanation could be this factor that gives the offset in the results from the reactor model compared to the pilot plant.

5.2.3 Validation of Rebased Model Against Pilot Plant with Modified Reaction Rate

To evaluate if the factor 2, detected in *5.1.3 Deshmukh Kinetic Model*, affects the results from the reactor model, an analysis was performed in this section. The reaction rates for reaction 1 and 2 were reduced by 50% in the reactor model and the results for the outlet composition and the temperature profile are presented below. Figure 17 shows the result with the modified reactor model for the outlet composition of the main products and in Table 8, the relative deviation is presented, both for the modified and unmodified reactor model.

Outlet Composition of Main Components with Modified Reaction Rate

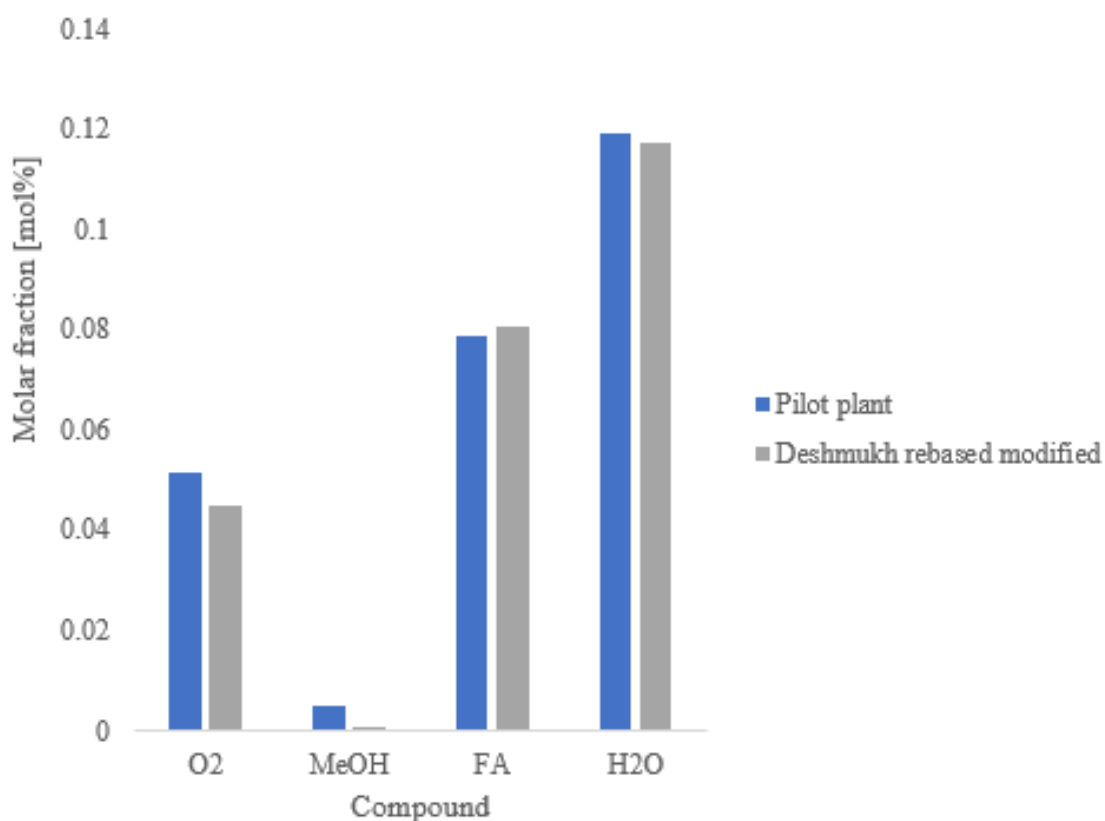


Figure 17: Validation against pilot reactor of the outlet composition of the main components.

Table 8: Calculated deviation of the outlet composition, with modified reaction rate, for the main components.

Compound	Relative Deviation Compared to Pilot Plant Data for the Unmodified Reactor Model [%]	Relative Deviation Compared to Pilot Plant Data for the Modified Reactor Model [%]
<i>O₂</i>	-19	-12
<i>MeOH</i>	-95	-89
<i>FA</i>	-5.6	+2.6
<i>H₂O</i>	+3.6	-1.8

As Figure 17 and Table 8 shows, the deviation for all the main component were decreased when reaction rate 1 and 2 were modified. Oxygen and methanol show

a lower molar fraction than expected, the same behaviour as in Figure 14. With the modified reaction rates, the molar fraction of formaldehyde and water shows different behaviour compared with the unmodified version. The modified reactor model produces more formaldehyde and less water compared to the pilot plant data. The outlet composition for the side products for the modified reactor model can be seen in Figure 18 and the relative deviation can be seen in Table 9. The relative deviation for the reactor model without the modification were also added in Table 9 for comparison.

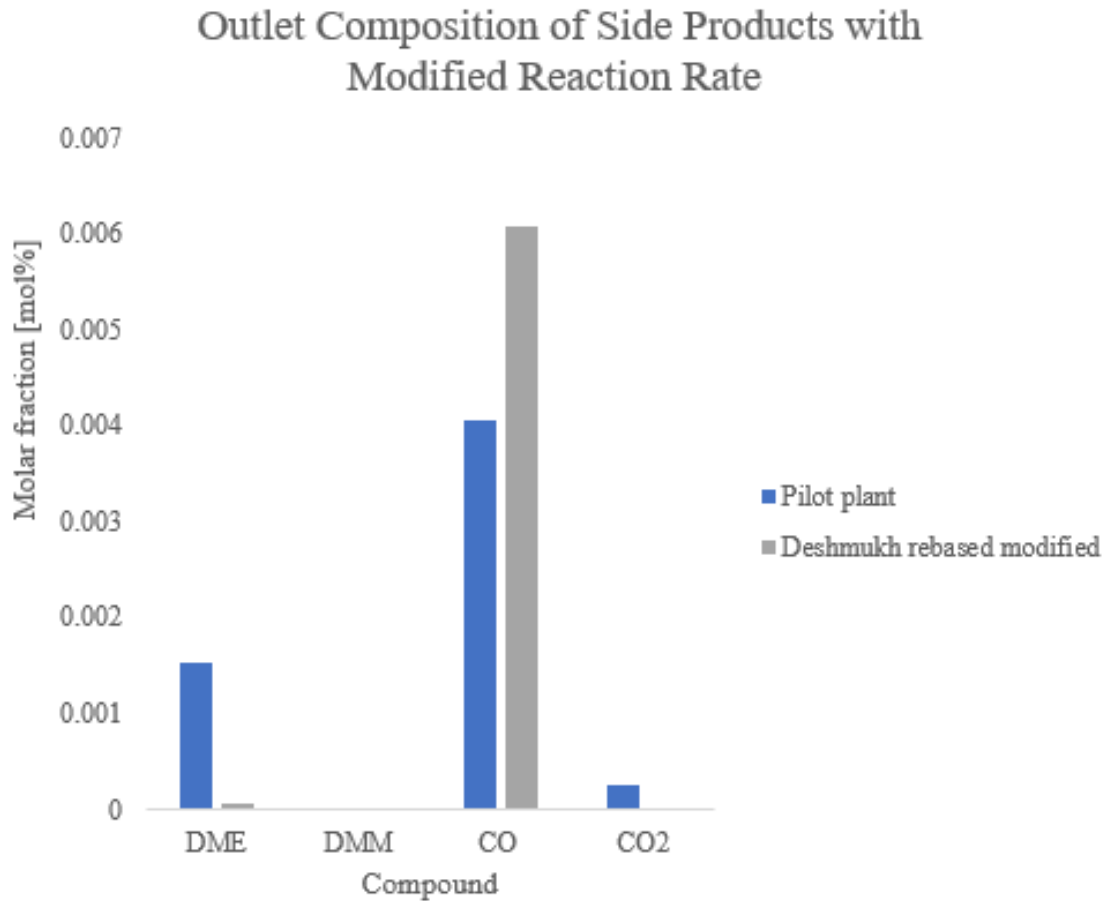


Figure 18: Validation against pilot reactor of the outlet composition of the side products.

Table 9: Calculated deviation of the outlet composition, with the modified reaction rate, for the side products.

Compound	Relative Deviation Compared to Pilot Plant Data for the Unmodified Reactor Model [%]	Relative Deviation Compared to Pilot Plant Data for the Modified Reactor Model [%]
<i>DME</i>	-99	-97
<i>DMM</i>	0	0
<i>CO</i>	+212	+50
<i>CO₂</i>	-100	-100

The result of the outlet composition from the reactor model with the modified reaction rates presented in Figure 18, shows a decreased deviation compared to the pilot plant, than the unmodified version. As seen in Table 9, the relative deviation of *CO* was decreased to +50% compared to +212% with the unmodified reactor model. The result in Figure 18 still shows an increase of reaction rate for reaction 2 compared to the pilot reactor. It is also possible to observe slightly improvement in the *DME* concentration, with -97% relative deviation instead of -99% before the modification. No variation was observed for *DMM* because of 0 output concentration and no variation for *CO₂* since this reaction rate was not added in the reactor model. The temperature profile seen in Figure 19, shows the same behaviour for the three evaluated data sets.

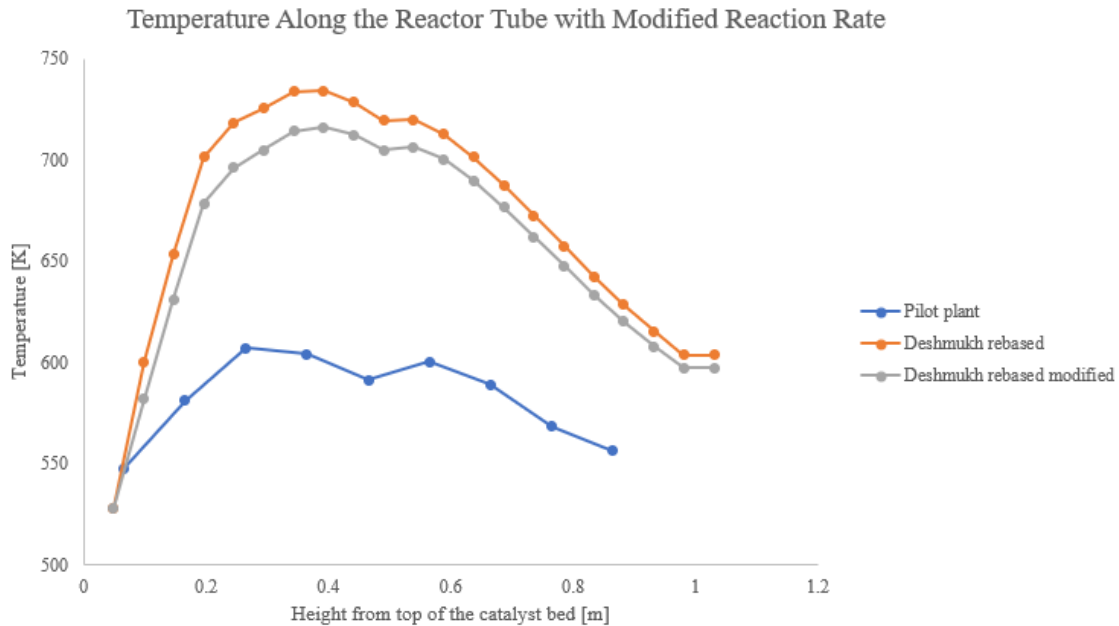


Figure 19: Validation against pilot reactor of the temperature profile.

The reactor model with the modified reaction rates, has a lower temperature

than the unmodified reactor model. The deviation in temperature is smaller for the modified reactor model compared with the pilot plant data. The lowered temperature obtained with the modified reactor model, could be explained by a decrease of reaction rate 1 and 2, since the reaction enthalpy are higher for these reactions compared to the rest.

The modified reactor model has a lower molar fraction of methanol and oxygen than expected compared with the pilot plant data. A possible explanation could be a higher reaction rate for reaction 1 in the reactor model compared to the pilot reactor. The formaldehyde production is higher with the modified reactor model compare to the pilot reactor, which aligns with the explanation of a higher reaction rate for reaction 1. The production of *CO* is higher then expected compared to the pilot plant and indicates a higher reaction rate of reaction 2 as well. The conclusion with a higher reaction rate for reaction 1 and 2 applies on the modified reaction rate as well as the unmodified version. Improvements of the results regarding the outlet composition was observed with the modified reactor model. Although when the modified reactor model was compared with the pilot plan data, the reaction rates for reaction 1 and 2 were still higher than expected. The relative deviation of the outlet composition between the reactor model and the pilot plant data was decreased for all the components and the temperature was decreased as well.

5.2.4 Validation of 2D model

The reactor model was developed as a 2D model and the outlet composition and the temperature profile along the tube was evaluated in the radial direction in this section. To define the radial direction in the reactor model, the radius was divided into 10 points where the first point was defined in the middle of the reactor. The results from ACM, was taken from the first radial point describing the center of the tube and the last radial point, describing the properties at the wall.

The outlet composition for all the compounds simulated in the model are shown in Table 10. The composition in the middle of the tube was compared with the composition at the wall of the reactor tube.

Table 10: Comparison of outlet composition between the center and the middle of the reactor tube.

Compound	Outlet composition in the middle [mol%]	Outlet composition at the wall [mol%]
H_2	0	0
N_2	7.477e-1	7.477e-1
O_2	4.136e-2	4.136e-2
CO	1.268e-2	1.268e-2
CO_2	0	0
H_2O	1.238e-1	1.238e-1
$MeOH$	2.122e-4	2.122e-4
FA	7.427e-2	7.427e-2
DME	5.925e-6	5.927e-6
DMM	0	0

As seen in Table 10, the composition is almost exactly the same for all compounds at the wall and in the middle. This result implies that the reaction rates are similar across the radial direction of the tube.

In Figure 20, the temperature profile along the reactor tube is plotted, both in the center of the reactor tube and at the wall.

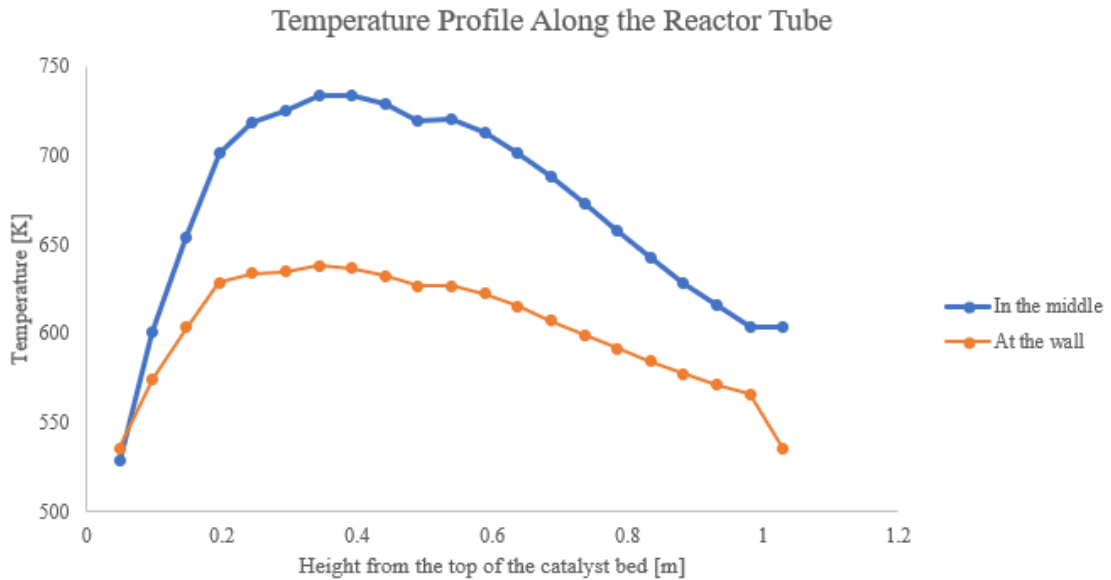


Figure 20: Comparison of the temperature profile along the reactor tube, between the center and the middle of the reactor tube.

As shown in Figure 20, the temperature profiles have a similar shape. Independent of the position in the radial direction, the hot spots are obtained at the same

height. A lower temperature was received at the wall compared to the temperature in the center of the reactor tube. This is explained by the heat transfer fluid cooling the reactor tube from the outside of the tube. The high temperature of the gas in the middle of the tube are due to the exothermic reactions taking place. The heat transfer fluid acts as a cooling jacket surrounding the reactor tube and will not be able to cool the gas in the middle of the tube as much as the gas closer to the wall. As discussed above in *5.2.2 Validation of Rebased Model Against Pilot Plant*, the higher temperature achieved by the reactor model could be caused by the heat transfer resistance through the wall. The gas fluid close to the wall should have a similar value to the cooling temperature, but it deviated with around 100°C in this case. This indicates a problem with the cooling of the gas flow and is probably caused by the heat transfer resistance.

In Figure 21, the temperature gradient was plotted. The radial direction was defined from the center of the reactor tube and the radius was divided into 10 points to describe the radial direction. The graph shows the decrease in temperature from the middle of the tube to the wall, as expected and discussed above in this section.

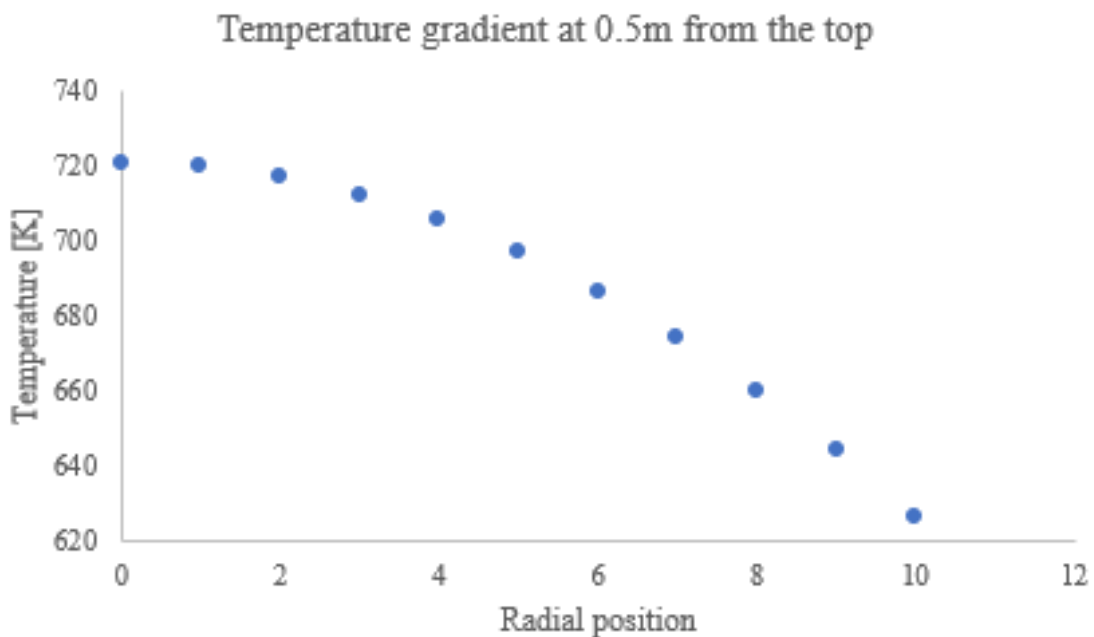


Figure 21: Temperature gradient from the middle of the tube to the wall, at a height of 0.5m from the top of the catalyst bed.

In *Appendix A*, the temperature gradient is shown for three different points along the reactor tube in order to evaluate if the behaviour is constant along the reactor tube. The same behaviour was observed in all the three plots, showing a temperature decrease from the middle of the tube to the wall and indicates a similar behaviour along the tube.

The composition and the temperature are showing expected results when the output are evaluated at different radial positions. It can be concluded that the

reaction rates are well described in the reactor model - in both axial and radial direction.

5.3 General Discussion

The power law kinetics, used in *Version 1* and *Version 2*, caused numerical errors when using pilot plant inputs. When the concentration of water was zero the program was not solving the equations since the reaction order of water was negative. Due to the numerical errors, another kinetic model was used, the Deshmukh kinetic model from literature [10]. *Version 3*, was implemented successfully to the reactor model and replaced the power law kinetics. *Version 3*, was validated against the literature paper, described in *5.1.3 Deshmukh Kinetic Model* and the result indicated a correct implementation in ACM. In order to validate the reactor model against the pilot plant data, *Version 4* was rebased with a reference temperature and experimental data provided by Schmidt [13] was used to refit a new parameter set.

The rebased kinetic model was implemented in the reactor model and the code was converged and run in steady state. The results from the model in Aspen, shown in *5.2.2 Validation of Rebased Model Against Pilot Plant*, showed some deviation from the pilot plant data. The same behaviour were obtained, with hot spots on the same height in the tube and the outlet concentration of the main component was in the same range as the pilot plant data. The temperature profile obtained a higher value when simulated in ACM then expected and the outlet compositions indicated a higher reaction rate of reaction 1 and 2. As discussed above in *5.2.2 Validation of Rebased Model Against Pilot Plant*, the explanation to the higher temperature and the offset of the outlet concentration can be explained by a higher reaction rate of reaction 1 and 2 and a decreased reaction rate of the rest of the reactions. Another possible explanation is the kinetic parameters, which are based on experimental data from literature and is not fully applicable on the reaction taking place in the pilot reactor. More tests has to be performed against the pilot plant data to identify the deviation from the pilot plant data.

To better describe the pilot plant, *Version 4 - b* should be used. The kinetic parameters in this version was refitted to the experimental data from Schmidt [13] and the operation conditions, such as pressure, temperature, catalyst type, was adjusted to describe the pilot reactor. The refitted model was tested in ACM as well but this model was not converging in the same way as the rebased one. More time has to be invested in this convergence problem and evaluate if the program can converge with the refitted kinetic parameter set. It might be necessary to collect more experimental data from the small-scale reactor in order to obtain more accurate kinetic parameters.

Due to the time limit of this project, the mass and heat transfer limitations internal to the pellet, were not implemented in the reactor model. In order to get a accurate result from the reactor model, this has to be done as a future work. The development and the implementation of the kinetic model as well as the validation

against the pilot plant was prioritized in this project. A lot of time was spent to calculate the correct parameters and match the operation conditions describing the pilot reactor, to get the model prepared for the validation against the pilot reactor.

6 Conclusion

When the project started, the power law kinetics was used to describe the reactions taking place in the reactor. At an early stage it was observed that numerical errors occurred with this model and Deshmukh kinetic model [10] replaced the power law kinetics. *Version 4 - a* was validated against the pilot plant and this kinetic model showed a good potential to describe the pilot reactor since the deviation are relatively small and it follows the expected behaviour. The results from *5.1.3 Deshmukh Kinetic Model* showed a deviation of the reaction rates for reaction 1 and 2 with a factor 2, compared to the literature results. The kinetic model *Version 4 - a*, was modified and the reaction rates for reaction 1 and 2 were decreased by 50% to evaluate how this factor affected the results from the reactor model.

The outlet composition of oxygen and methanol was lower than expected when compared with the pilot plant data showed for both the modified and unmodified rebased reactor model. Oxygen and methanol are mainly consumed in reaction 1 and a higher reaction rate of reaction 1 can be a possible explanation to the observed result. The outlet composition of *CO* showed a relative deviation of +212% compared to the pilot plant data with the unmodified rebased model from Deshmukh [10]. With the modified reactor model, the relative deviation of *CO* was decreases to 50%. A higher concentration of *CO* can be explained by a higher reaction rate of reaction 2, since this is the only reaction forming this side product.

The reactor model obtained a higher temperature compared to the pilot plant data but the a similar temperature profile was obtained, both for the modified and unmodified rebased reactor model. This result can be explained by the higher reaction rates of reaction 1 and 2 and it could also be caused by the heat transfer resistance though the wall. With the modified reactor model, the relative deviation decreased when comparing the outlet composition with the pilot plant data and the temperature profile was improved as well with a relative deviation of +15% with the modified reactor model compared to +18% with the unmodified.

Expected behaviour was obtained when an analysis was performed in the radial direction of the reactor tube. The outlet composition was constant in the radial direction and the temperature decreased from the center of the tube to the wall. The different catalyst layers were described and implemented in the reactor model as well and the inert dilution was considered.

To conclude, the kinetic models was implemented successfully and valuable results were obtained when validating the rebased kinetic model against the pilot plant data. The structure of Deshmukh kinetics [10] was implemented and if the kinetic parameters are to be changed further on, it can be done easily using this model.

The reactor model shows a good potential and an expected behaviour compared to the pilot reactor.

6.1 Future Work

In order for the reactor model to describe the pilot plant, further work has to be done on the reactor model. Considering the kinetic model, the refitted model has to be evaluated. The convergence problem can be evaluated and it might require new experimental data to regress a new parameter set, if the current one cannot converge. In this project, the same kinetic model was assumed to describe the different layers along the reactor tube. To improve the accuracy of the kinetic model, different parameter sets can be regressed for the different catalysts used in the reactor.

To improve the reactor model itself, the internal mass and heat transfer limitations has to be implemented in the reactor model. This will be done by adjusting the existing external mass and heat transfer equations and express it as one global mass respectively heat transfer equation.

References

- [1] Gerberich, H.R; Seaman, G.C. 2013. *Formaldehyde*. Kirk-Othmer Encyclopedia of Chemical Technology. Online via: <https://onlinelibrary-wiley-com.ludwig.lub.lu.se/doi/10.1002/0471238961.0615181307051802.a01.pub3> [2021-02-22]
- [2] Sigma-Aldrich. 2021. *Formaldehyde solution*. Online via: <https://onlinelibrary-wiley-com.ludwig.lub.lu.se/doi/10.1002/0471238961.0615181307051802.a01.pub3> [2021-02-22]
- [3] Johnson Matthey. 2021 **FORMOX 2.0**. Online via: <https://matthey.com/en/products-and-services/chemical-processes/licensed-processes/formox-2> [2021-02-22]
- [4] Andersson, A; Holmberg, J; Häggblad, R. Johnson Matthey Formox. 2016. *Process Improvements in Methanol Oxidation to Formaldehyde: Application and Catalyst Development*. in Springer Science + Business Media New York.
- [5] Viegaard Raun, K; Johannessen, J; McCormack, K; Clausen Appel, C; Baier, S; Thorhauge, M; Høj, M; Degn Jensen, A. *Modeling of the molybdenum loss in iron molybdate catalyst pellets for selective oxidation of methanol to formaldehyd*. in Chemical Engineering Journal 361.
- [6] Young-Deuk, K; Woo-Seung, K; Youngjin, L. 2015. *Influences of exhaust gas temperature and flow rate on optimal catalyst activity profiles*. International Journal of Heat and Mass Transfer.
- [7] Aspen Tech. 2004. *Modeling Language Reference Guide*. Aspen Custom Modeler 2004.1.
- [8] Spatenka, S; Matzopoulos, M; Urban, Z; Cano, A. 2019. *From Laboratory to Industrial Operation: Model-Based Digital Design and Optimization of Fixed-Bed Catalytic Reactors*. Industrial & Engineering Chemistry Research.
- [9] Höst, M; Regnell, B; Runesson P. 2006 *Att genomföra examensarbete*. Studentlitteratur, Lund.
- [10] Deshmukh, S.A.R.K.; van Sint Annaland, M.; Kuipers, J.A.M. 2005 *Kinetics of the partial oxidation of methanol over a Fe-MO catalyst*. Faculty of Science and Technology, University of Twente, Netherlands. Science Direct.
- [11] Berger, R, J; Hugh Stitt, E; Marin, G, B; Kapteijn, F; Moulijn, J, A. 2001 *Chemical reaction kinetics in practice*. Cat-Tech, Syntex, Cleveland USA, Euronokin.
- [12] Axelsson, S. 2015 *The impact of water on the partial oxidation of methanol over a FeMo-catalyst*. Chemical Engineering, Lund Univeristy.

- [13] Schmidt, M. 2020. *Towards an intrinsic kinetic model for the partial oxidation of methanol using a MeFe-catalyst*. Department of Chemical Engineering, Lund University.
- [14] Deutschmann, O; Knözinger, H; Kochloeff, K; Turek, T. 2011 *Heterogeneous Catalysis and Solid Catalysts, 1*. Fundamentals. Ullmann's Encyclopedia of Industrial Chemistry. Online via: https://onlinelibrary-wiley-com.ludwig.lub.lu.se/doi/10.1002/14356007.a05_313.pub3 [2021-02-26]
- [15] Vannice, M. A. 2007 *An analysis of the Mars-van Krevelen rate expression*. Department of Chemical Engineering, Pennsylvania State University, University Park, PA 16802, United States.
- [16] Fogler, H, S. 2017 *Diffusion and Reaction*. Elements of Chemical Reaction Engineering, Chapter 15.
- [17] Berger, R. 2010. *EUROKIN spreadsheet on requirements for measurement of intrinsic kinetics in the gas-solid fixed-bed reactor*. DelftChemTech, Delft University of Technology, Netherlands.
- [18] Ross, J R-H. 2019. Contemporary Catalysis, Chapter 8: *Mass and Heat Transfer Limitations and Other Aspects of the Use of Large-Scale Catalytic Reactors*. Elsevier B.V.
- [19] Fogler, H, S. 2017 *Mass Transfer Limitations in Reacting Systems*. Elements of Chemical Reaction Engineering, Chapter 14.
- [20] Alveteg, M. 2017. *Handbook*. Department of Chemical Engineering, Faculty of Engineering, Lund University.
- [21] Harrysson, P. 2021 *Picture of pilot reactor*. Email-conversation, Johnson Matthey Formox AB.
- [22] Häggblad, R. 2021. *Catalyst calculations, Teams meeting*. R&D Manager at Johnson Matthey Formox AB.
- [23] Kisko, K. 2021. *Catalyst calculations, Teams meeting*. Senior Scientist at Johnson Matthey Formox AB.
- [24] Taskinen, E; Taskinen, A. 2008 *Proximity effects of oxygen atoms on the enthalpies of formation of simple diethers: a computational G3(MP2)//B3 study*. Journal of Physical Organic Chemistry
- [25] Gallen, R. 2021. *Meeting regarding kinetic development*. Senior Scientist at Johnson Matthey.
- [26] GraphReader.com. 2021 *Graph Reader*. Online via: <http://www.graphreader.com/> [2021-04-05]

Appendix A

In this appendix, the temperature gradient between the center and the wall are plotted at three different positions along the reactor tube. The radial position starts at 0 in the center of the tube and the radius was divided into 10 points to receive the radial positions.

In Figure 22, the temperature gradient is shown at a height of 0.3m from the top of the catalyst bed.

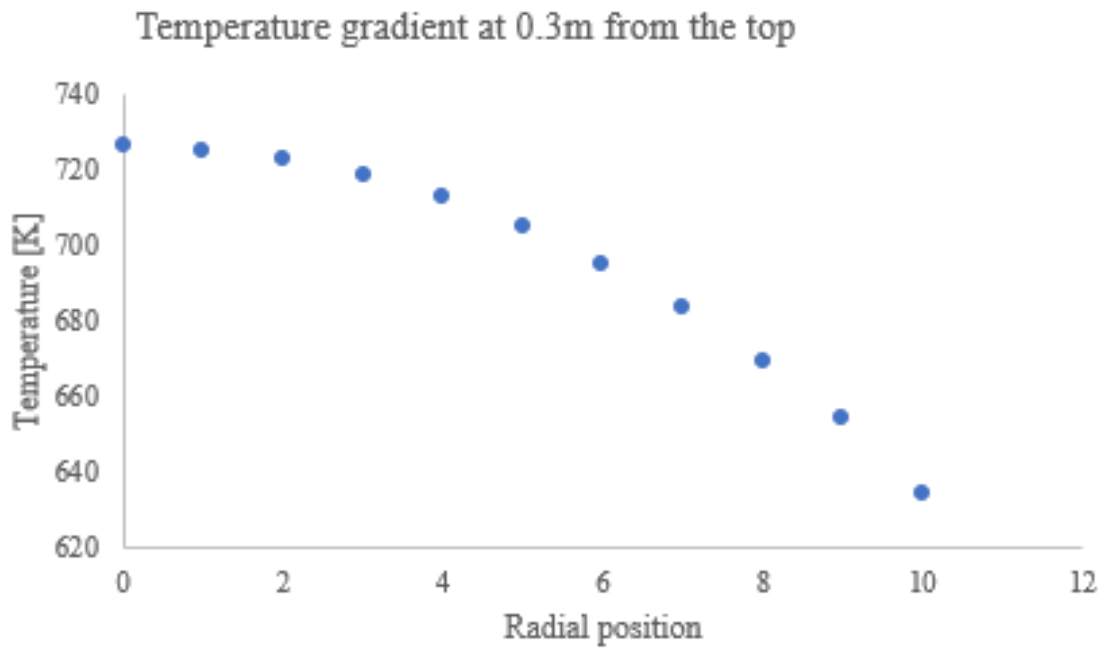


Figure 22: Temperature gradient from the middle of the tube to the wall, at a height of 0.3m from the top of the catalyst bed.

In Figure 23, the temperature gradient is shown at a height of 0.5m from the top of the catalyst bed.

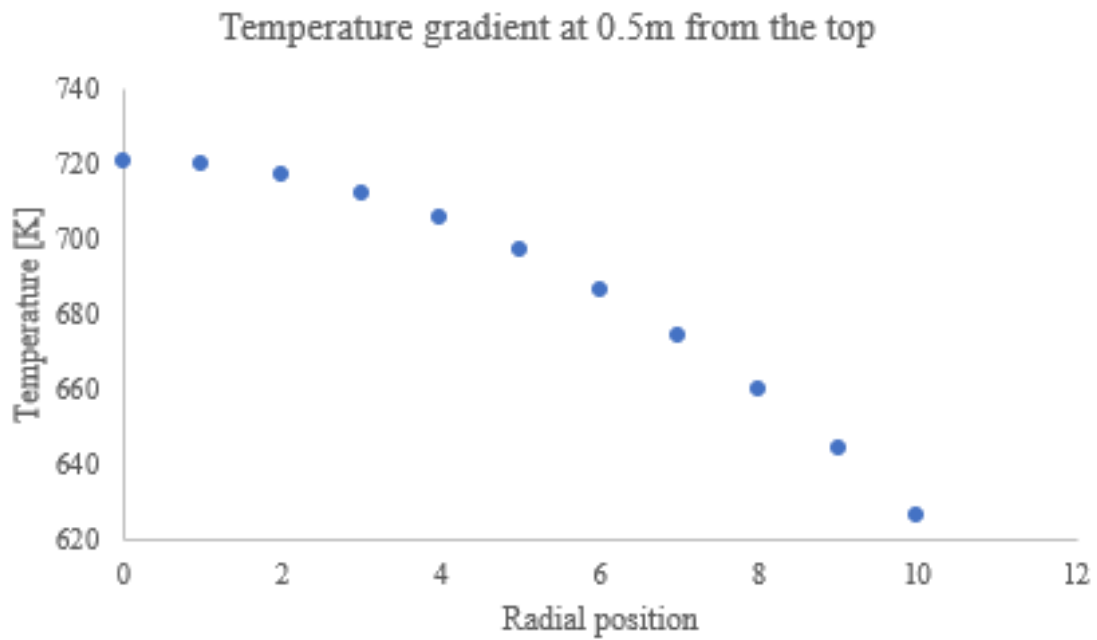


Figure 23: Temperature gradient from the middle of the tube to the wall, at a height of 0.5m from the top of the catalyst bed.

In Figure 24, the temperature gradient is shown at a height of 0.8m from the top of the catalyst bed.

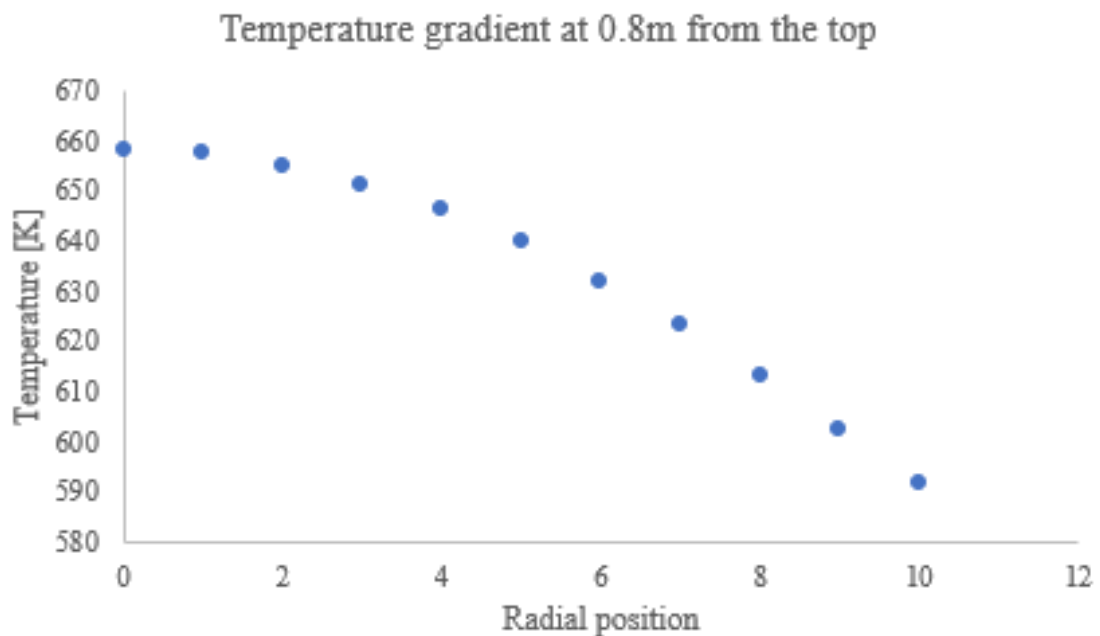


Figure 24: Temperature gradient from the middle of the tube to the wall, at a height of 0.8m from the top of the catalyst bed.